

Seasonal variability in gaseous mercury fluxes and mercury deposition to dew

Amber Diane Converse  
Whitewater, WI

B.A., Macalester College, 2004

A Thesis presented to the Graduate Faculty  
of the University of Virginia in Candidacy for the Degree of  
Master of Science

Department of Environmental Science

University of Virginia  
December, 2009

*Goda Kando*

---

*Manuel Tendler*

---

*Hufnagel*

---

# TABLE OF CONTENTS

## Chapter 1

|     |                   |   |
|-----|-------------------|---|
| 1.1 | Introduction..... | 1 |
| 1.2 | References.....   | 4 |

## Chapter 2

|     |  |    |
|-----|--|----|
| 2.1 | Seasonal variability in gaseous mercury fluxes measured in a<br>high-elevation meadow..... | 7  |
| 2.2 | Figures.....   | 25 |
| 2.3 | Tables.....  | 30 |
| 2.4 | Supplemental Information.....  | 32 |
| 2.5 | References.....  | 40 |

## Chapter 3

|     |  |    |
|-----|--|----|
| 3.1 | Seasonal contribution of dewfall to mercury deposition determined<br>using a micrometeorological technique and dew chemistry sampling..... | 48 |
| 3.2 | Figures.....   | 64 |
| 3.3 | Tables.....  | 68 |
| 3.4 | References.....  | 70 |

## Chapter 4

|     |  |    |
|-----|--|----|
| 4.1 | Conclusions and avenues for future research..... | 73 |
| 4.2 | References.....                                  | 78 |

## **CHAPTER 1**

### **Introduction**

---

Atmospheric elemental mercury (Hg) can be effectively transported around the globe with reports of measureable concentrations in atmospheric and aquatic environments far from point sources (Nriagu and Pacyna, 1988; Fitzgerald et al., 1998). Once the metal is deposited to land or water surfaces, it can be transformed by sulfur-reducing bacteria (Morel et al., 1998) into the neurotoxin methylmercury (MeHg). The toxin bioaccumulates in the food chain resulting in high concentrations in predatory fish and other high-trophic level organisms (Wolfe et al., 1998). Atmospheric Hg concentrations measured within ice-cores increased 20-fold from preindustrial times (prior to the 1840s) to the mid-1980s (Schuster et al., 2002). Since the 1990s, however, concentrations have declined to an 11-fold increase likely due to reductions in anthropogenic emissions. As of 2008, the Environmental Protection Agency (EPA) has established fish consumption advisory warnings across all 50 states for streams, rivers, and lakes (U.S. Environmental Protection Agency, 2009). Understanding the fundamentals of Hg cycling is necessary in order to regulate Hg emissions in the future, and predict regions where Hg toxicity is likely to be a concern.

Mercury is unique among metals in that it is a liquid at standard temperature and pressure. The elemental form has a high ionization potential ( $241 \text{ kcal mol}^{-1}$ ), greater than that of noble metals (e.g. Ag, Pd, and Pt) and comparable to the inert gas Ra ( $248 \text{ kcal mol}^{-1}$ ) (Schroeder et al., 1991). This may account for the larger fraction of atmospheric Hg in the elemental form (>95%, Schroeder and Munthe, 1991; Poissant et al., 2005). Hg is commonly divided into three operationally defined species: gaseous elemental mercury (GEM), gaseous oxidized mercury (GOM, comprised of any species containing  $\text{Hg}^{2+}$ ), and particulate-bound mercury ( $\text{Hg}_p$ ). Background GEM concentrations typically range from  $1.5\text{-}1.8 \text{ ng m}^{-3}$  (Valente et al., 2007) but can reach levels  $>20 \text{ ng m}^{-3}$  in highly polluted regions (e.g. Liu et al., 2002). The ionized GOM species can be considered “sticky” and binds to most surfaces including sample line tubing. Because of GOM’s high reactivity and the inherently low atmospheric concentrations, instrumentation has only recently been developed for continuous atmospheric measurements of the GOM and  $\text{Hg}_p$  species. The relative abundance of these two species varies by location, but typically accounts for only a few percent of the total Hg (Poissant et al., 2005).

Atmospheric Hg can be entrained in rainfall or fog (wet deposition) or deposited directly from the atmosphere (dry deposition). Dry deposition can be of equal magnitude or greater than wet deposition processes (Lyman et al., 2007). Any deposited Hg can subsequently be emitted back to the atmosphere as GEM or remain in the terrestrial or aqueous environments where it can be sorbed to soils, stored in plant and animal tissues, or dissolved in water (Lindberg et al., 2007).

Efforts to better understand regional and global Hg cycling are compounded by the limited number of seasonal datasets. As of 2009, the Mercury Deposition Network (MDN) has 114 active sites around the United States that collect weeklong rainfall-composite samples to monitor wet deposition variability (National Atmospheric Deposition Program, 2009). Plans are currently underway to set up a similar sampling network for speciated atmospheric Hg concentrations (Tim Sharac, EPA, personal communication). Studies of atmospheric Hg fluxes (deposition and emission) are limited to individual sampling efforts of researchers, which usually translates into short-term studies restrained to a single season. Atmospheric Hg fluxes are thought to be dependent on numerous factors including temperature (Wallschläger et al., 1999), precipitation patterns (Lindberg et al., 1999; Song and Van Heyst, 2005), vegetation cover including plant age and community composition (Lindberg et al., 1998; Fritsche et al., 2008), incident light (Moore and Carpi, 2005), and the levels atmospheric oxidants (Engle et al., 2005). Many of these variables exhibit a high degree of seasonality that affect regional Hg cycling.

The goal of my research was to better understand some of the seasonal components of Hg dynamics and was divided into two projects: (1) seasonal *in situ* GEM fluxes over a terrestrial landscape, and (2) seasonal Hg deposition to dew. Results from each experiment was written as an independent article for publication, and therefore, the introductory material incorporates some repetition. The first project (Chapter 2) explores how atmospheric GEM deposition/emission varies across seasons at a remote, vegetated site in Shenandoah National Park, Virginia. The second project (Chapter 3) addresses the seasonal contribution of dew to Hg deposition and its relative significance in comparison to other depositional pathways. The final chapter (Chapter 4) summarizes the major conclusions from my work and highlights potential avenues for future mercury research.

**REFERENCES: INTRODUCTION**

- Engle, M. A., M. S. Gustin, S. E. Lindberg, A. W. Gertler, and P. A. Ariya (2005), The influence of ozone on atmospheric emissions of gaseous elemental mercury and reactive gaseous mercury from substrates, *Atmospheric Environment*, 39(39), 7506-7517.
- Fitzgerald, W. F., D. R. Engstrom, R. P. Mason, and E. A. Nater (1998), The case for atmospheric mercury contamination in remote areas, *Environmental Science & Technology*, 32(1), 1-7.
- Fritsche, J., D. Obrist, M. J. Zeeman, F. Conen, W. Eugster, and C. Alewell (2008), Elemental mercury fluxes over a sub-alpine grassland determined with two micrometeorological methods, *Atmospheric Environment*, 42(13), 2922-2933.
- Lindberg, S., R. Bullock, R. Ebinghaus, D. Engstrom, X. B. Feng, W. Fitzgerald, N. Pirrone, E. Prestbo, and C. Seigneur (2007), A synthesis of progress and uncertainties in attributing the sources of mercury in deposition, *Ambio*, 36(1), 19-32.
- Lindberg, S. E., P. J. Hanson, T. P. Meyers, and K. H. Kim (1998), Air/surface exchange of mercury vapor over forests - The need for a reassessment of continental biogenic emissions, *Atmospheric Environment*, 32(5), 895-908.
- Lindberg, S. E., et al. (1999), Increases in mercury emissions from desert soils in response to rainfall and irrigation, *Journal of Geophysical Research-Atmospheres*, 104(D17), 21879-21888.
- Liu, S. L., F. Nadim, C. Perkins, R. J. Carley, G. E. Hoag, Y. H. Lin, and L. T. Chen (2002), Atmospheric mercury monitoring survey in Beijing, China, *Chemosphere*, 48(1), 97-107.
- Lyman, S. N., M. S. Gustin, E. M. Prestbo, and F. J. Marsik (2007), Estimation of dry deposition of atmospheric mercury in Nevada by direct and indirect methods, *Environmental Science & Technology*, 41(6), 1970-1976.
- Moore, C., and A. Carpi (2005), Mechanisms of the emission of mercury from soil: Role of UV radiation, *Journal of Geophysical Research-Atmospheres*, 110(D24).
- Morel, F. M. M., A. M. L. Kraepiel, and M. Amyot (1998), The chemical cycle and bioaccumulation of mercury, *Annual Review of Ecology and Systematics*, 29, 543-566.

- National Atmospheric Deposition Program (2009), NADP Program Office, Illinois State Water Survey, 2204 Griffith Dr., Champaign, IL 61820.
- Nriagu, J. O., and J. M. Pacyna (1988), Quantitative assessment of worldwide contamination of air, water and soils by trace metals, *Nature*, 333(6169), 134-139.
- Poissant, L., M. Pilote, C. Beauvais, P. Constant, and H. H. Zhang (2005), A year of continuous measurements of three atmospheric mercury species (GEM, RGM and Hg-p) in southern Quebec, Canada, *Atmospheric Environment*, 39(7), 1275-1287.
- Schroeder, W. H., G. Yarwood, and H. Niki (1991), Transformation processes involving mercury species in the atmosphere – results from a literature survey, *Water Air and Soil Pollution*, 56, 653-666.
- Schroeder, W. H., and J. Munthe (1998), Atmospheric mercury - An overview, *Atmospheric Environment*, 32(5), 809-822.
- Schuster, P. F., D. P. Krabbenhoft, D. L. Naftz, L. D. Cecil, M. L. Olson, J. F. Dewild, D. D. Susong, J. R. Green, and M. L. Abbott (2002), Atmospheric mercury deposition during the last 270 years: A glacial ice core record of natural and anthropogenic sources, *Environmental Science & Technology*, 36(11), 2303-2310.
- Song, X. X., and B. Van Heyst (2005), Volatilization of mercury from soils in response to simulated precipitation, *Atmospheric Environment*, 39, 7494-7505.
- U.S. Environmental Protection Agency (2009), Fish Advisories Technical Fact Sheet: 2008 Biennial National Listing, edited.
- Valente, R. J., C. Shea, K. L. Humes, and R. L. Tanner (2007), Atmospheric mercury in the Great Smoky Mountains compared to regional and global levels, *Atmospheric Environment*, 41(9), 1861-1873.
- Wallschläger, D., R. R. Turner, J. London, R. Ebinghaus, H. H. Kock, J. Sommar, and Z. F. Xiao (1999), Factors affecting the measurement of mercury emissions from soils with flux chambers, *Journal of Geophysical Research-Atmospheres*, 104(D17), 21859-21871.

Wolfe, M. F., S. Schwarzbach, R. A. Sulaiman, and Yu (1998), Effects of mercury on wildlife: A comprehensive review, *Environmental Toxicology and Chemistry*, 17(2), 146-160.

## CHAPTER 2

# Seasonal variability in gaseous mercury fluxes measured in a high-elevation meadow

---

### Abstract

Seasonal patterns of atmospheric mercury (Hg) fluxes measured over vegetated terrestrial systems can provide insight into the underlying process controlling emission and deposition of Hg to vegetated surfaces. Gaseous elemental Hg fluxes were measured for week-long periods in each season (spring, summer, fall, and winter) over an uncontaminated high-elevation wetland meadow in Shenandoah National Park, Virginia using micrometeorological methods. Mean net deposition was observed in the spring ( $-4.8 \text{ ng m}^{-2} \text{ h}^{-1}$ ), emission in the summer ( $2.5 \text{ ng m}^{-2} \text{ h}^{-1}$ ), near zero flux in the fall ( $0.3 \text{ ng m}^{-2} \text{ h}^{-1}$ ), and emission in the winter ( $4.1 \text{ ng m}^{-2} \text{ h}^{-1}$ ). Nighttime deposition (when stomata are closed) and the poor correlation between Hg fluxes and canopy conductance during periods of active vegetation growth suggest that stomatal processes are not the dominant mechanism for ecosystem-level GEM exchange at this site. The strong springtime deposition relative to summer implies that young vegetation is better at scavenging Hg, with the highest deposition occurring at night possibly via a cuticular pathway.

## 1. Introduction

Mercury (Hg) is recognized as a global pollutant with background atmospheric concentrations in the Northern Hemisphere typically ranging from 1.5-1.8 ng m<sup>-3</sup> (Valente et al., 2007). There is a growing body of literature addressing the major pathways that couple Hg in the atmospheric, terrestrial, and aquatic systems (e.g. Schroeder and Munthe, 1998; Grigal, 2002; Lindberg et al., 2007). A broad seasonal record of Hg deposition and emission is necessary to understand the processes governing Hg fluxes over terrestrial systems (Gustin et al., 2008). However, there is currently a paucity of seasonal datasets collected over vegetated landscapes. Several studies have targeted a single season, often summer (e.g. Lindberg et al., 1998; Marsik et al., 2005; Schroeder et al., 2005; Obrist et al., 2006; Fritsche et al., 2008b), while very few (such as Lindberg et al., 2002 and Fritsche et al., 2008a) report measurements across multiple seasons. Among these studies, Hg fluxes are widely variable in both magnitude and direction, and because of site specific differences (e.g. Hg soil and air concentrations, vegetation type and age, local Hg sources) it is a challenge to discern seasonal patterns by compiling individual studies.

Understanding the mechanisms behind ecosystem-level Hg fluxes can also provide insight into broader regional patterns. For example, Obrist (2007) suggested that the seasonal differences in atmospheric Hg concentrations observed in the Northern Hemisphere could be linked to vegetation dynamics. The lower Hg concentrations in the summer could be partially attributed to plant uptake. In the winter, higher Hg concentrations could be related to increased fossil fuel combustion, Hg being emitted back to the atmosphere from plant decomposition, or dormant plants not actively scavenging Hg. Before interpreting Hg fluxes at the ecosystem-level, it is helpful to briefly review the current understanding of Hg emission and deposition pathways from vegetation and soil, individually.

Plants are known to accumulate Hg in their above-ground biomass over the growing season (Rea et al., 2002; Ericksen et al., 2003; Frescholtz et al., 2003; Fay and Gustin, 2007; Bushey et al., 2008). Three major pathways have been proposed for Hg distribution within plants and for the observed Hg fluxes over vegetation. First, plants could take up Hg from the soil via their roots, transport it to the above ground tissue, and emit it through stomata (Hanson et al., 1995; Lindberg et

al., 1998). Support for this hypothesis has been restricted to wetland species with physical structures, such as lacunal space, that facilitate transport of gaseous compounds from the root system (Lindberg et al., 2002; Poissant et al., 2004b; Lindberg et al., 2005). For other forms of vegetation, however, Hg concentrations in leaves are usually weakly correlated or independent of the soil Hg concentration (Erickson et al., 2003; Frescholtz et al., 2003; Fay and Gustin, 2007). Second, atmospheric Hg could enter leaves through stomata with the direction of the flux determined by a concentration gradient (inside vs. outside the stomata, Browne and Fang, 1978; Lindberg et al., 1992). This often-invoked mechanism has been challenged by the results from a recent chamber study in which the degree of stomatal opening was controlled. In this experiment, stomatal conductance was not found to have an effect on the measured foliar exchange of Hg (Stamenkovic and Gustin, 2009). Finally, Hg could adsorb to the cuticle where it can be subsequently washed off, released back to the atmosphere, or remain bound within the plant tissue. Any xenobiotic, such as Hg, could penetrate the cuticle via a lipophilic or non-lipophilic pathway depending on its chemical properties. The lipophilic pathway operates by a molecule adsorbing to the cuticle lipids, diffusing through the membrane, and ultimately sorbing to the epidermal cells (Buchholz, 2006). A non-lipophilic pathway to transport inorganic ions and charged organics has been proposed via aqueous polar pores (Schreiber, 2005). Neither of these pathways has been specifically addressed for Hg.

Bare soils exhibit bidirectional Hg fluxes based on factors such as underlying geology (Gustin et al., 1999; Xin and Gustin, 2007), the extent of historic atmospheric Hg deposition (Xin et al., 2007), radiation (Moore and Carpi, 2005; Xin et al., 2007; Xin and Gustin, 2007), temperature (Wallschläger et al., 1999), soil saturation (Lindberg et al., 1999; Song and Van Heyst, 2005), atmospheric oxidants (Engle et al., 2005), and the atmospheric Hg concentration (Xin and Gustin, 2007). Numerous studies have reported diel cycles in soil Hg emissions that are positively correlated with solar radiation (e.g. Carpi and Lindberg, 1997; Engle et al., 2001; Zhang et al., 2001) and temperature (e.g. Gustin et al., 1997; Poissant and Casimir, 1998; Zhang et al., 2001). However, it has been noted that the diel cycling in Hg emissions continues even when soils are held at a constant temperature in the dark when outside ambient air is used as the flushing gas (Zhang et al., 2008). This suggests that another

atmospheric constituent that also follows a diel cycle, such as ozone, can control Hg emissions from soils.

A seasonal approach can help to characterize the processes governing Hg exchange over a mixed soil and vegetation surface. Assuming that the vegetation is dormant in the winter, the measured Hg flux during this period can be attributed to the soils alone. Observations in the spring, summer, and fall can highlight how the change in vegetation form and function can affect the magnitude and direction of the Hg flux. In keeping with this overall approach, the specific objectives of this study are to: (1) quantify Hg fluxes over a terrestrial landscape on a seasonal basis over the course of a year, (2) determine if Hg fluxes exhibit distinct seasonal patterns, and (3) use seasonal differences, diurnal variability, and correlations to other environmental parameters to infer possible Hg emission/deposition pathways associated with vegetated terrestrial surfaces.

## 2. Experimental Methods

Atmospheric Hg is typically categorized into three species with different chemical and physical properties that affect their behavior and reactivity: gaseous elemental Hg (GEM,  $\text{Hg}^0$ ) comprising >95% of total atmospheric Hg (Poissant et al., 2005), gaseous oxidized Hg (GOM, any gaseous compound involving  $\text{Hg}^{2+}$ ), and particulate-bound Hg ( $\text{Hg}_p$ ). The instrumentation used to quantify atmospheric Hg in this study (ambient air analyzer, Tekran 2537b) is designed to measure GEM, the concentrations and fluxes of which we report here.

### 2.1 Site description

Four approximately week-long field campaigns were conducted from August 6-12, 2008 (hereafter called summer), November 5-14, 2008 (fall), February 9-17, 2009 (winter), and May 11-19, 2009 (spring). GEM fluxes were measured at a high-elevation wetland meadow in Shenandoah National Park, VA referred to as Big Meadows (Figure 1). There was very little continuous open water at the site, but soils remained near saturation for much of the study period. The meadow is an open, relatively flat area consisting of low lying non-woody vegetation, with the dominant species being sedges (*Carex spp.*), lowbush blueberry (*Vaccinium pallidum*), bent grass (*Agrostis capillaris*), poverty oatgrass (*Danthonia spicata*), whorled loostripe (*Lysimachia quadrifolia*), maleberry (*Lyonia*

*ligustrina*), and hayscented fern (*Dennstaedtia punctilobula*) (Wendy Cass, personal communication).

The meadow is bordered by primarily deciduous forest on all sides. The canopy height reached approximately 0.6 m in the summer and fell to 0.3 m in the winter (consisting of senesced, above-ground growth from the previous season). Big Meadows typically experiences warm and humid summers, mild winters with limited snow coverage, and an annual precipitation of ~1300 mm (Lawrence and Hornberger, 2007). A Mercury Deposition Network (MDN) rainfall sampling station, which has been in operation since late 2002, is situated approximately 700 m north of the site. The mean Hg concentration in rainfall for the Oct 2002-Dec 2008 period is  $8.80 \pm 7.08 \text{ ng L}^{-1}$  (National Atmospheric Deposition Program (NRSP-3), 2009). Water samples collected from a standing pool in the center of the meadow (May, 2009) had an average Hg concentration of  $4.09 \text{ ng L}^{-1}$ . Water Hg concentrations further downstream are substantially lower with a mean of  $0.60 \text{ ng L}^{-1}$  (Moore, 2007). Soils in the meadow have low Hg concentrations, containing  $0.10 \mu\text{g g}^{-1}$  ( $n = 2$ ) in the upper 0.05 m.

The National Park Service is actively managing Big Meadows with mow/burn/fallow treatments to support native species and control the growth of woody plants. The managed area is divided into three approximately equal sections (western/central/eastern, Figure 1), and within the year of our measurement, the western section was mowed in the winter and the eastern section was burned (March 24, 2009). The spring measurement occurred several weeks after the controlled burn when the new vegetation had emerged.

A portable flux tower was placed in the central portion of the meadow ( $38^{\circ}30'54'' \text{ N}$ ,  $78^{\circ}26'04'' \text{ W}$ ) to ensure adequate fetch. A small patch of woody vegetation was situated directly east of the tower, and therefore data with wind directions from  $30^{\circ}$  to  $150^{\circ}$  were removed from the dataset (less than 5% of all measurements). The dominant wind direction is typically west or southwest, and the footprint for most atmospheric measurements fell within the central section.

## 2.2. Micrometeorological methodology

Micrometeorological techniques to measure the air-surface exchange of trace gasses offer numerous advantages: they do not disturb the environment to capture true *in situ* conditions, they record continuously, and they represent fluxes averaged over a large surface area. Several types of

gradient techniques have been used to determine GEM fluxes from surfaces (e.g., Lindberg et al., 1995; Cobos et al., 2002; Edwards et al., 2005). These approaches are based on the theory that the flux is proportional to the vertical gradient of the scalar, as:

$$F_{GEM} = -K_{GEM} \frac{\partial C_{GEM}}{\partial z} \quad (1)$$

where  $F_{GEM}$  is the flux of GEM ( $\text{ng m}^{-2} \text{s}^{-1}$ ),  $K_{GEM}$  is the eddy diffusivity ( $\text{m}^2 \text{s}^{-1}$ ), and  $\partial C_{GEM} / \partial z$  is the concentration gradient of GEM ( $\text{ng m}^{-4}$ ) (Baldocchi et al., 1988). Two common techniques to determine the eddy diffusivities are the aerodynamic method and modified Bowen ratio (MBR) method, and we used both for comparison purposes within this study. According to micrometeorological convention, deposition is defined as a negative flux while emission is a positive.

The aerodynamic method is based in Monin-Obukov similarity theory where under specific conditions (e.g. horizontally homogenous surface layer) vertical gradient measurements can be related to fluxes. Accounting for atmospheric stability,  $F_{GEM}$  can be calculated from measurements at two heights above a surface according to:

$$F_{GEM} = \frac{ku_* (\bar{C}_1 - \bar{C}_2)}{\ln\left(\frac{z_1 - d}{z_2 - d}\right) - \psi_{GEM1} - \psi_{GEM2}} \quad (2)$$

where  $k$  is the von Kármán constant (0.4),  $u_*$  is the friction velocity ( $\text{m s}^{-1}$ ),  $z_1$  and  $z_2$  are the two inlet heights (m),  $d$  is the zero plane displacement height (approximated as 2/3 canopy height, m),  $\bar{C}_1$  and  $\bar{C}_2$  are the mean GEM concentrations at heights  $z_1$  and  $z_2$  ( $\text{ng m}^{-3}$ ), and  $\psi_{GEM1}$  and  $\psi_{GEM2}$  are the integrated scalar similarity functions at heights  $z_1$  and  $z_2$ . The integrated similarity functions are dependent on atmospheric stability, which is determined from the Obukov length,  $L$  (Brustear, 1982). Eddy covariance measurements of sensible and latent heat fluxes are used in the calculation of  $L$ . Additional information regarding the assumptions of this method and applications to trace gas fluxes can be found in Baldocchi et al. (1988) with the more specific application to GEM fluxes in Edwards et al. (2005).

The MBR method does not rely on stability corrections while assuming similarity with other scalars. The concentration of a reference scalar (sensible heat or another trace gas) can be measured at the same heights as the GEM, and the gradient calculated. We chose to use water vapor as the

reference trace gas since its instrumentation was readily available for measurements at the two heights.

Eddy covariance with fast response sensors for water vapor can determine the flux directly ( $F_{H_2O}$ ),

allowing for the calculation of the eddy diffusivity of the reference,  $K_{H_2O}$ :

$$K_{H_2O} = -\frac{F_{H_2O}}{\Delta\bar{C}_{H_2O}/\Delta z} \quad (3)$$

where  $\Delta\bar{C}_{H_2O}$  is the mean water vapor concentration gradient at heights  $z_1$  and  $z_2$  ( $\text{kg m}^{-3}$ ). If the

sources and sinks of the reference gas are the same, then eddy diffusivity of GEM is the same as that

of the reference scalar, and the flux of GEM is calculated as follows:

$$F_{GEM} = -K_{H_2O} \frac{\Delta\bar{C}_{GEM}}{\Delta z} = F_{H_2O} \frac{\Delta\bar{C}_{GEM}}{\Delta\bar{C}_{H_2O}} \quad (4)$$

Both of the previously described MM methods have assumptions and associated limitations that should be noted. First, the measured fluxes represent a spatial average from the area within the tower footprint. The size of this footprint changes based on the height of the instrumentation and atmospheric conditions (i.e. wind direction, wind speed, etc). Therefore, inherent to any gradient technique, the footprints of the two measurement heights will be different. Second, the concentration gradient of GEM (and water vapor for the MBR method) needs to be great enough to be accurately differentiated by the instrumentation. This is particularly challenging for remote, uncontaminated areas where gradients of GEM are typically low. There is the option of removing data where the GEM gradient is below a method detection limit (MDL), but this is often not done since it would eliminate small flux measurements resulting in an exaggerated mean flux (e.g. Fritsche et al., 2008a). Specific to the MBR method, calculated GEM fluxes can be significantly overestimated when the gradient of water vapor becomes very small, often during transition periods (dawn and dusk). Finally, both methods require adequate turbulence, which is often not the case at night when wind speeds are low. Fortunately, the field site in this study was relatively windy in both the day and night with  $u_*$  values consistently above  $0.1 \text{ m s}^{-1}$  for over 92% of the entire measurement period.

One of the proposed pathways for GEM to enter and leave plant tissue is via the stomata, and therefore the GEM fluxes could be related to stomatal conductance ( $g_{st}$ ). Rather than attempting to continually measure this at our site, we arrive at this indirectly through the calculation of the bulk

canopy conductance ( $g_c$ ) with respect to water vapor. For this, we use a rearranged version of the Penman-Monteith equation (Monteith and Unsworth, 1990):

$$g_c = \left[ \left( \frac{\Delta}{\gamma} \right) \left( \frac{R_n - G}{\lambda E} - 1 \right) (1/g_a) + \frac{\rho_a c_p D_a}{\gamma \lambda E} \right]^{-1} \quad (5)$$

where  $\Delta$  is the slope of the saturation vapor pressure curve as a function of air temperature (mb K<sup>-1</sup>),  $\gamma$  is the psychrometric constant (mb K<sup>-1</sup>),  $R_n$  is the net radiation (W m<sup>-2</sup>),  $G$  is the soil heat flux (W m<sup>-2</sup>),  $\lambda$  is the latent heat of vaporization (J kg<sup>-1</sup>),  $c_p$  is the specific heat of air (J kg<sup>-1</sup> K<sup>-1</sup>),  $g_a$  is the aerodynamic conductance (m s<sup>-1</sup>), and  $D_a$  is the vapor pressure deficit (mb). The aerodynamic conductance was calculated as:

$$g_a = \left[ \frac{\left[ \ln \left( \frac{z-d}{z_{om}} \right) - \psi_m \right] \left[ \ln \left( \frac{z-d}{z_{ov}} \right) - \psi_v \right]}{k^2 u_r} \right]^{-1} \quad (6)$$

where  $z_{om}$  and  $z_{ov}$  are the momentum and scalar (water vapor) roughness lengths (m),  $\psi_m$  and  $\psi_v$  are the momentum and scalar stability corrections, and  $u_r$  is the wind speed at the reference height (m s<sup>-1</sup>) (Monteith and Unsworth, 1990).

#### 2.4 Instrumentation

A ~4 m portable flux tower was erected at the same location within the meadow for each short-term campaign. Sensible heat, latent heat, CO<sub>2</sub>, and H<sub>2</sub>O fluxes were determined using a triaxial sonic anemometer (CSAT3, Campbell Scientific, Inc.) in tandem with an open path H<sub>2</sub>O and CO<sub>2</sub> analyzer, placed 2.41 m above the ground (Li7500, Li-Cor, Inc.). Components of net radiation (CNR1, Kipp and Zonen), total ultraviolet radiation (TUVR, Eppley), and photosynthetic photon flux density (LI190SB Quantum Sensor, Campbell Scientific, Inc.) were measured on site. Temperature and relative humidity were measured at two heights (1.31 m and 3.05 m) housed in naturally aspirated radiation shields (HMP45c, Campbell Scientific, Inc.). Two calibrated soil heat flux plates (HFT3-L, Campbell Scientific, Inc.) were buried at a depth of 0.05 m at the base of the tower in tandem with a total of four glass-insulated thermocouples (two at 0.025 m and two at 0.075 m depth, Omega Engineering, Inc.). Volumetric soil moisture content was measured at two locations using water content reflectrometers (CS616-L, Campbell Scientific, Inc.) and a leaf wetness sensor attached to the base of the tower at approximately canopy height indicated the presence of dew or substantial fog

(LWS-L, Decagon Devices). Rain events were recorded with a tipping bucket rain gauge located approximately 2 m from the tower. Data from all the above instrumentation was recorded on a data logger (CR23X, Campbell Scientific, Inc.) and averaged to 20 minutes to match GEM gradient measurement intervals. Power was supplied by a 3000W gasoline generator which was refilled twice per day (EU3000IS, Honda). The generator was situated ~15 m east of tower, downwind of the dominant wind direction so combustion emissions would not interfere with the atmospheric measurements. Hourly ozone measurements were taken at the nearby National Park Service air quality monitoring station.

GEM concentrations were measured at two heights (1.31 m and 3.05 m) using an ambient air analyzer (2537b, Tekran, Inc.) equipped for dual sampling. Briefly, the analyzer operates by drawing the sample air over a gold trap, which preferentially binds to Hg, for a 5-minute sampling interval with a flow rate of  $1.25 \text{ L min}^{-1}$ . The Hg is then thermally desorbed from the gold trap for analysis by cold vapor atomic fluorescence spectrometry with an instrument detection limit of  $< 0.1 \text{ ng m}^{-3}$  (Tekran, Inc.). The analyzer is equipped with two gold cartridges to allow for continuous sampling (i.e. one cartridge actively trapping Hg from the sample air while the other is undergoing analysis). Signal bias between the gold cartridges is accounted for by sampling twice from each inlet height before switching to the other inlet resulting in one GEM gradient measurement every 20 minutes. All tubing was made of Teflon to reduce adsorption to the inner walls and the ~35 ft sample lines are insulated and heated to  $50^\circ\text{C}$  to inhibit water condensation that could induce Hg deposition. Particulate filters ( $0.2 \mu\text{m}$ ) were located at each sample inlet and immediately in front of the analyzer. Alternate sampling of the dual lines was controlled by two solenoids and a solenoid controller (1110 Synchronized Two Port Sampling System, Tekran) in tandem with a small external pump (Micro Diaphragm Gas Pump, KNF Neuberger, Inc.). One inlet line fed to the Hg analyzer while ambient air was pulled through the other by the external pump to ensure a constant air flow through both lines.

Sample lines and filters were checked for contamination before and after the entire sampling regime by flushing with Hg-free air created by a zero air generator (model 1100, Tekran, Inc.). The Hg analyzer was calibrated daily by an internal  $\text{Hg}^0$  permeation source. In addition, manual

calibrations, completed by injecting a known volume of Hg<sup>0</sup> (2505 calibration unit, Tekran, Inc.), were conducted before and after sampling periods to confirm the accuracy of the permeation source. Particulate filters for the sample lines were replaced at the beginning of each sampling period.

The Hg sampling equipment was housed in a 48 inch steel storage box fitted with two computer fans to maintain air circulation and a flat panel heater regulated by a temperature controller. In the fall, winter, and spring seasons when the temperatures began to drop more substantially, the entire box was relocated inside a heavy-duty tent to maintain warm temperatures. A power conditioner was used for all of the Hg-analyzer equipment to reduce power fluctuations from the generator. The battery back-up capability of the conditioner also allowed for continuous measurements while refilling the generator with gasoline.

### **3. Results**

#### *3.1 Data coverage and post-processing*

Valid concentrations and fluxes of GEM covered 75% of the total measurement period across the four seasons. Data gaps resulted from the initial set-up phase when the Hg-analyzer had not warmed-up, power failures, instrument malfunction, and daily calibrations. Rain and fog caused the Li7500 to malfunction, a persistent problem in the fall when misty conditions often prevailed. All measurements and subsequent calculations derived from the Li7500 were removed if the vapor pressure deficit deviated more than 20% from the average measurements made by the two relative humidity probes. GEM fluxes were not further time averaged to remove variability, as done in other studies (Fritsche et al, 2008a; Fritsche et al, 2008b), due to the short-term nature of the sampling periods.

Webb-Pearman-Leuning (WPL) corrections were applied to account for the changing air density due to differences in atmospheric water vapor (Webb et al., 1980). Axis rotations were also applied to correct for any minor instrument misalignment (McMillen, 1988). Statistical analyses were conducted using SPSS Statistics 17.0 (SPSS, Inc.) and Matlab R2008b (The Mathworks). A one-way analysis of variance (ANOVA) was used to compare sample means, and a student's t-test determined if flux measurements were statistically different from zero. Statistical relationships were

assumed significant at  $p < 0.05$ . Any subsequent use of the  $\pm$  symbol indicates the standard deviation from the mean.

### *3.2 Seasonal meteorological conditions*

Environmental conditions were highly variable across the four seasons, as expected for a high-elevation site (Table 1). Numerous thunderstorms developed in the spring, fair weather dominated in the summer, fog often persisted in the fall, while strong winds and light snow occurred in the winter. The dominant wind was southwest in the summer and west in the fall and winter. In the spring, wind directions were more variable ranging from northwest to southeast.

### *3.3 GEM concentrations*

GEM concentrations (determined from the upper inlet) remained relatively constant with a mean of  $1.29 \pm 0.10 \text{ ng m}^{-3}$  over the entire measurement period, similar to those seen at other remote locations ( $0.99 - 2.35 \text{ ng m}^{-3}$ ; Valente et al., 2007). There were no significant trends in GEM concentrations within each sampling period (Figure 2), and no apparent association with wind direction (data not shown). The highest mean GEM concentration occurred in the winter, consistent with numerous other studies that report higher concentrations during this season (e.g., Ebinghaus et al., 2002; Mao et al., 2008). Correlation coefficients for GEM levels with other meteorological parameters are listed in Table 2.

### *3.4 GEM fluxes*

#### *3.4.1 GEM fluxes: Evaluation of techniques and variability*

GEM fluxes calculated using the aerodynamic method were comparable to those determined using the MBR method, particularly in the spring and summer (Table 1). However, when the water vapor gradient between the two measurement heights was minimal (due to low rates of evapotranspiration) the flux determined with the MBR method resulted in large standard deviations in calculated fluxes (see equation 8 and Table 2). This led to poor agreement between the two methods during the fall and winter seasons. The aerodynamic method, which does not rely on water vapor gradients, did not demonstrate this behavior, and was therefore considered more reliable. All future discussions of GEM fluxes reference the results based on this technique.

Bidirectional GEM fluxes were calculated for all seasons and exhibited a high degree of variability ranging from  $-125.7$  to  $119.1 \text{ ng m}^{-2} \text{ h}^{-1}$  (Table 1). The large standard deviations are likely attributed to the small GEM gradient typical of a remote site and are consistent with other MM GEM flux measurements that did not apply temporal averaging techniques (e.g. Marsik et al., 2005; Poissant et al., 2004b) which have the effect of smoothing this variability.

#### 3.4.2 GEM fluxes: Correlations to environmental parameters

Correlations between GEM fluxes with other meteorological variables were generally weak ( $|\rho| < 0.40$ ) and were not consistent in magnitude or direction between seasons (Table 2). In the spring, GEM fluxes were significantly correlated with temperature (air and soil), all measured forms of shortwave radiation,  $\text{CO}_2$  concentration, and water vapor flux. These parameters were also significantly correlated in the summer season, in addition to volumetric soil moisture, wind speed, relative humidity, and  $\text{CO}_2$  flux. In general, summer exhibited the strongest correlations with measured meteorological variables. The GEM fluxes during the fall season were poorly correlated with the majority of parameters except GEM concentration, relative humidity, and  $\text{CO}_2$  flux. In the winter, GEM fluxes were significantly correlated with GEM concentrations and all forms of shortwave radiation.

Volumetric soil moisture was only significantly correlated in the summer, while ozone and daytime  $g_c$  were not significantly correlated to GEM fluxes during any season. In dry soils, soil moisture is often positively correlated with GEM fluxes from soils, and large emissions have been observed after precipitation events (Lindberg et al., 1999). However, this relationship is not as significant when soils are near saturation (Song and Van Heyst, 2005), as was the case in Big Meadows. Increasing ozone levels have been seen to effect GEM fluxes over terrestrial surfaces in laboratory studies (Engle et al., 2005), but this pattern was not observed at our site (data not shown). Early GEM flux research over a plant canopy suggested that enhanced stomatal closure during drought conditions could reduce GEM emissions, implying that ecosystem-level fluxes could be partially stomatal controlled (Lindberg et al., 1998). The poor correlation with daytime canopy

conductance in the vegetated seasons suggests that the measured GEM fluxes at this site are not governed by stomatal opening.

### 3.4.3 GEM fluxes: Net seasonal fluxes

Distinct seasonal differences were observed in the average GEM fluxes. Deposition dominated in the spring ( $\bar{F}_{GEM} = -4.8 \text{ ng m}^{-2} \text{ h}^{-1}$ ), emission in the summer ( $\bar{F}_{GEM} = 2.5 \text{ ng m}^{-2} \text{ h}^{-1}$ ), near zero flux in the fall ( $\bar{F}_{GEM} = 0.3 \text{ ng m}^{-2} \text{ h}^{-1}$ ), and emission in the winter ( $\bar{F}_{GEM} = 4.1 \text{ ng m}^{-2} \text{ h}^{-1}$ ). A time series of cumulative GEM fluxes displays these patterns (Figure 3). Although many of the individual GEM gradient measurements were near the detection limit of the analyzer, these cumulative plots reveal any upward or downward bias in the measured fluxes. Inherent to any short term campaign, the trends seen during each condensed sampling period might not be representative of patterns for the entire length of each season. Average fluxes in the spring, summer, and winter were all statistically different from zero ( $p < 0.05$ ), but the average fall GEM flux was not ( $p = 0.75$ ).

### 3.4.4 GEM fluxes: Diurnal patterns

In the summer, GEM fluxes were significantly greater in the daytime than in the nighttime with mean values of  $6.5$  and  $-2.5 \text{ ng m}^{-2} \text{ s}^{-1}$ , respectively (where daytime is defined as periods where incident short wave radiation was greater than  $5 \text{ W m}^{-2} \text{ s}^{-1}$ ). This pattern was not significant in any other season ( $p = 0.052, 0.34, \text{ and } 0.10$  for the spring, fall, and winter, respectively). However, it was noted that increased deposition/reduced emission was apparent in all nighttime fluxes relative to daytime (Table 1).

At the hourly scale, GEM fluxes in the summer effectively tracked all types of incident shortwave solar radiation (total shortwave, UV, and PAR; Figure 4), transitioning from small net deposition at night to net emission during the day. A similar pattern is visible in the spring with smaller daytime emission peaks and enhanced nighttime deposition. The fall GEM fluxes did not exhibit a noticeable diel pattern. In the winter, fluxes remained near zero at nights and then increased midday.

## 4. Discussion

Seasonal trends in GEM fluxes captured using the MM approach at a single site offer insight into the naturally occurring eco-system level processes which incorporate both vegetation, soil and water dynamics without the interference of an experimentally altered environment. The site had very few open pools of water; therefore we will limit the discussion to soil and vegetation.

#### *4.1 Seasonality of GEM fluxes*

Significant differences in GEM fluxes were observed between seasons, with emission dominating the winter (dormant season), transitioning to deposition in the spring (early growing season), followed by small emissions in the summer (late growing season), and no significant flux during fall (senescence). In theory, with vegetation dormant, Hg fluxes in winter should represent soil fluxes with minimal vegetation effects. In fact, we find that Hg fluxes observed in winter are comparable in magnitude and direction to numerous measurements over uncontaminated bare soil in any season (Figure 5). Stamenkovic et al. (2008) also noted that winter GEM fluxes over a combination soil and dry plant stubble were approximately equal to fluxes measured over bare soil. Low levels of Hg in the soil that have accumulated from years of wet and dry deposition consistently emit Hg back into the atmosphere when atmospheric GEM concentrations are low. The differences in emission magnitude between sites are likely attributed to a combination of environmental parameters including temperature, wind speeds, canopy coverage, and solar radiation. While soil fluxes likely vary in magnitude throughout the seasons at our site, we assume that they will always be emission fluxes and similar to wintertime magnitudes when evaluating the rest of our seasonal data.

During the period of senescence in the fall season, we detected no measurable GEM flux. While vegetation is not actively growing, canopy coverage and the physical plant structure can remain as important factors. Two simple scenarios could explain the difference between fall and winter fluxes: (1) small Hg deposition to existing plant surfaces could offset soil emission fluxes or (2) soil fluxes are decreased due to light restriction from the plant structure. Kuiken et al. (2008b) noted that after senescence, when more light could reach surfaces beneath the canopy, soil emission fluxes increased. In addition, incident shortwave radiation and ozone concentrations were the lowest in the fall season,

and both of these parameters are related to Hg emissions from soils (Moore and Carpi, 2005; Engle et al., 2005).

The marked difference between the winter emission and spring deposition is likely due to uptake by the vegetation during the early period of growth. Plants are known to accumulate Hg from the atmosphere during the growing season (e.g. Rea et al., 2002; Erickson et al., 2003; Bushey et al., 2008), which translates into a depositional flux to the vegetation. GEM fluxes from soils are generally net emission in the spring (Figure 5), and since our site had an overall net deposition during this period, the downward flux to the vegetation overwhelms any upward flux from the soils.

The transition from spring deposition to summer emission implies that the uptake process by vegetation is reduced, that other emission pathways have increased (e.g. from the soil), or a combination of both factors. The first hypothesis has supporting evidence at the leaf scale. Poissant et al. (2008) measured GEM fluxes over enclosed maple tree foliage during the growing season. The GEM fluxes displayed a season-long, positive linear trend. Periods of early growth generally exhibited deposition fluxes which slowly transitioned to a mixture of emission/deposition in the fall, when plants were mature. Although foliar Hg concentrations increase over the growing season (Rea et al., 2002), the rate of uptake may be reduced as the plants age. For instance, Erickson et al. (2003) found that foliar Hg concentrations remained relatively constant in quaking aspen leaves after 2-3 months of growth. Variable rates of Hg uptake by plants may explain our observed ecosystem-level deposition in the spring (the high rate of Hg uptake into immature plants overwhelms emission from soil) in contrast to the ecosystem-level emission in the summer (emission from soil overwhelms the smaller rate of Hg uptake into mature plants). It is also possible that soil GEM fluxes increased in the summer. Temperature and incident solar radiation are important controls for soil emission fluxes (Moore and Carpi, 2005; Bahlmann et al., 2006), and both were greater in the summer.

Ecosystem scale evidence in support of Hg uptake by vegetation in the early growing season can be found in a study by Fritsche et al. (2008a). GEM fluxes were measured over grazed, managed grassland in Fruebuel, Switzerland. GEM deposition fluxes (of similar magnitude to our springtime

values) were observed in the spring and were maintained throughout the summer. The continuation of the deposition flux at Fruebuel into the summertime (in contrast to Big Meadows) may be attributed to vegetation management practices. The Fruebuel site was continually grazed and underwent regular grass cuts which could simulate continuous 'spring-like' growing conditions. At Big Meadows, the vegetation was only minimally grazed by wild deer and no grass cuts were completed during the summer months. A separate study at the Fruebuel site measured increased deposition immediately after the grass cut. However, this pattern was not visible at another site that also experienced a grass cut (Fritsche et al., 2008b). Other studies have measured net emissions over plant canopies during the summer as we observed in Big Meadows (e.g. Lindberg et al., 1998; Poissant and Casimir, 1998; Zhang et al., 2001; Schroeder et al., 2005).

#### *4.2 Evidence of a stomatal pathway?*

Our data suggest that daytime GEM fluxes over the mixed-vegetated surface were not limited by stomatal opening. Daytime canopy conductance was not significantly correlated to GEM fluxes in the spring or summer, the two seasons with actively growing vegetation. GEM fluxes also did not follow the typical diel pattern of stomatal conductance, which peaks midmorning before the daily solar maximum when temperatures are cooler and the vapor pressure deficit is lower. This differs from the diel profiles of radiation and temperature, which are relatively symmetrical and peak around solar noon.

It should be noted that the proposed stomatal pathway is also dependant on the ambient atmospheric concentration of GEM (e.g. lower ambient GEM levels could enhance emission processes). To account for this, we calculated the deposition velocity [ $\text{m s}^{-1}$ ] defined as the GEM flux over the ambient GEM concentration measured at the lower inlet height. Canopy conductance was not significantly correlated to the GEM deposition velocity in the spring or summer ( $p = 0.07$  and  $0.38$ , respectively). This suggests that: (1) the proposed stomatal pathway is not a dominant mechanism for ecosystem-level GEM exchange at our site, (2) GEM fluxes from stomata are not limited by canopy conductance, or (3) daytime emissions from other sources (e.g. soils) mask the

vegetation flux signal from stomata. Stamenkovic and Gustin (2009) noted that in controlled laboratory setting, reducing stomatal conductance did not affect the net Hg flux over enclosed plants.

#### 4.3 Alternative pathway for Hg exchange with vegetation

Investigating diurnal patterns offers an opportunity to evaluate the nonstomatal pathway in vegetation, because stomata are nearly closed during the night rendering that pathway inoperative. If the majority of the flux originating from the soil is emission (or near zero), then nighttime deposition fluxes during vegetated periods may be attributed to Hg scavenging by the plants through a cuticular pathway.

Age-related differences in the chemical and physical structure of vegetation could partially account for the differences between spring and summer GEM fluxes. The increased nighttime deposition in the spring relative to the summer could be attributed to the developing cuticle of the immature plants. The rate of development will vary depending on species and environmental parameters. As an example, Hauke and Schreiber (1998) noted that leaf area of ivy (*Hedera helix* L.) quickly increased for the first 30 days after bud-break. Isolated cuticle thickness increased more gradually and stabilized around 60-90 days. It is possible that in the early stages of growth a plant is more susceptible to xenobiotic uptake, and therefore could account for the enhanced GEM deposition. Alternatively, the plant tissue in the summer could be approaching equilibrium saturation with respect to GEM reducing the rate of uptake, as seen in non-polar organic pollutants (Riederer and Müller, 2006). A third possibility is that the changing cuticle structure with age could result in less deposition or enhanced emission of previously deposited GEM. The relative proportion of polar wax compounds in ivy (*Hedera helix* L.) cuticles was found to increase with increasing leaf age (Hauke and Schreiber, 1998). This process could reduce deposition velocities or promote re-volatilization of the non-polar GEM, as suggested for non-polar PCBs by Moeckel et al. (2008). Alternatively, spring nighttime temperatures were lower, and GEM emissions from the soil might have been of a smaller magnitude. Although each of these hypotheses is plausible, differentiating between them or unambiguously determining their importance relative to stomatal pathways will require further experimentation at the leaf level.

## 5. Summary and conclusion

In 2008-2009, we measured *in situ* GEM fluxes in Shenandoah National park using MM methods. GEM fluxes in this non-polluted site were bidirectional and variable across all seasons. Spring was characterized by net deposition, which transitioned to small net emissions in the summer, near zero fluxes in the fall, and larger net emissions in the winter. Daytime fluxes in the summer were significantly greater than nighttime values; this trend was also observed in all other seasons, but was not statistically significant. Correlations with other environmental parameters were generally weak and varied across seasons. There were no significant correlation with daytime  $g_c$  in the spring or summer, suggesting that GEM fluxes at our site are not controlled by a stomatal pathway. Assuming near zero or positive soil fluxes, the net nighttime deposition in the spring and summer supports the notion that deposition to vegetation can occur via a non-stomatal pathway.

Considering the large seasonal differences in GEM fluxes at one site, measurements made during one season will not provide an accurate basis for modeling GEM patterns at a larger scale. In light of this, additional work is needed to determine if our observations of seasonal GEM fluxes are representative of other locations and the duration of each seasonal emission/deposition pattern. Also, plant phenology could be important on a mechanistic level, with different processes influencing emission/deposition as plants develop. Observations of GEM fluxes over emergent vegetation are likely to be significantly different from those measured later in the growing season.

## Acknowledgments

This research was supported by the National Science Foundation and from the U.S. Department of Education's Graduate Assistance in Areas of National Need program. We'd like to thank Susie Maben, John Maben, and Clara Funk for their continuous support and advice, and several graduate and undergraduate students who assisted with field work: Karen Vandecar, Adam Benthem, Leslie Piper, Thushara Gunda, and Kelly Hokanson. Finally, we are very grateful to all of the Shenandoah National Park staff including Liz Garcia, Jim Schaberl, and Julena Campbell.

**Figure 1.** Map of the Big Meadows field site within Shenandoah National Park, VA. The white star indicates the location of the portable flux tower. The only major road within the park (Skyline Drive) is visible running from the NW to the NNE of the meadow. The white lines display the approximate divisions between the National Park Service management areas.

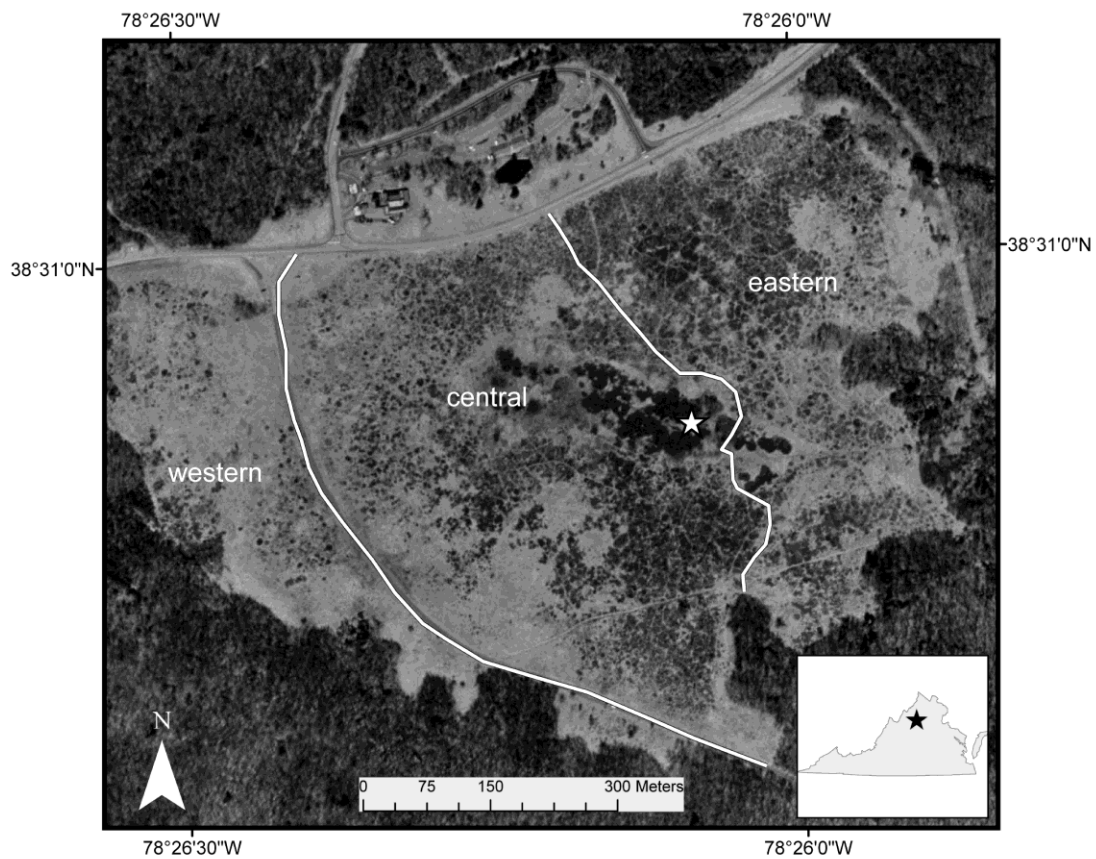


**Figure 2.** Time series measurements for each season. From top to bottom: GEM concentrations at the upper inlet [ $\text{ng m}^{-3}$ ], GEM fluxes [ $\text{ng m}^{-2} \text{h}^{-1}$ ] determined using the aerodynamic method, and  $\text{CO}_2$  flux [ $\mu\text{mol m}^{-2} \text{s}^{-1}$ ]. GEM concentrations remained relatively constant over all sampling periods while GEM fluxes exhibited a high degree of variability. The diel pattern in  $\text{CO}_2$  flux in the spring and summer indicates actively growing vegetation and microbial respiration.

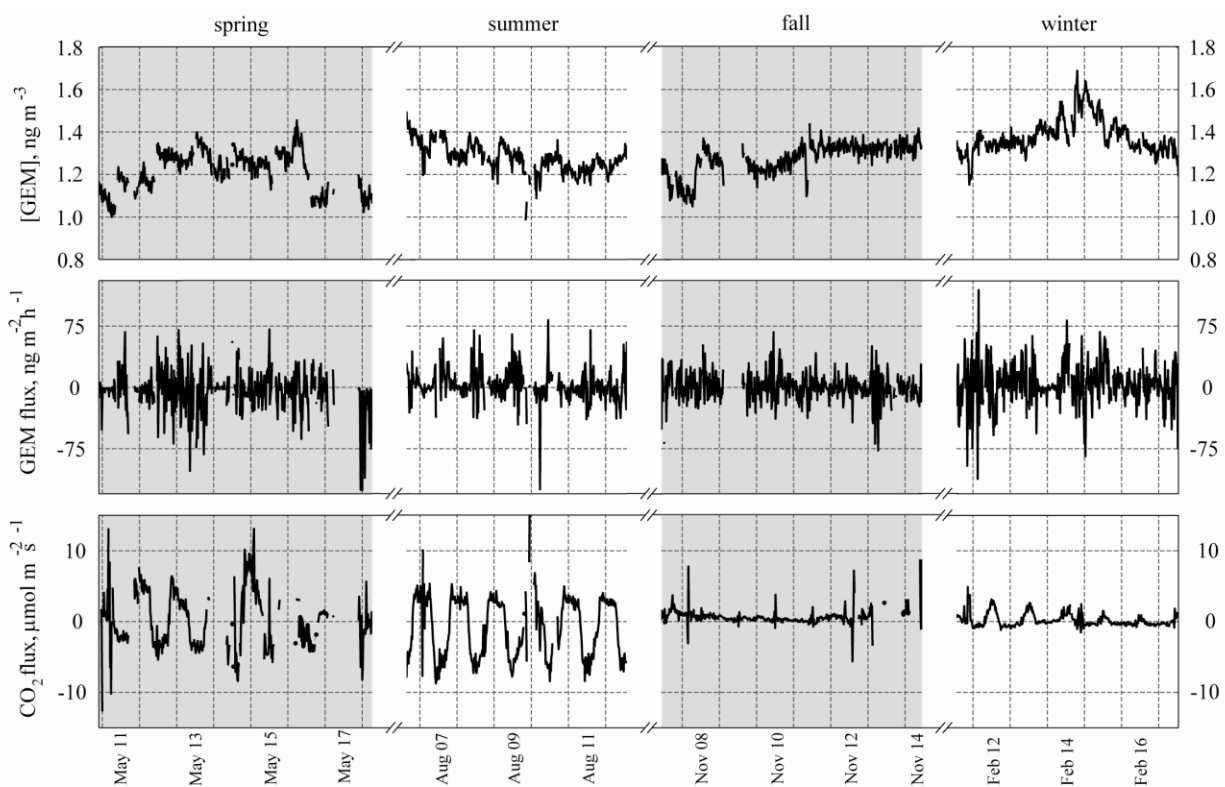


**Figure 3.** Time series cumulative GEM fluxes for each measurement period. Gaps in the GEM flux data were forced to zero and appear as gray horizontal lines (most noticeable in the spring).

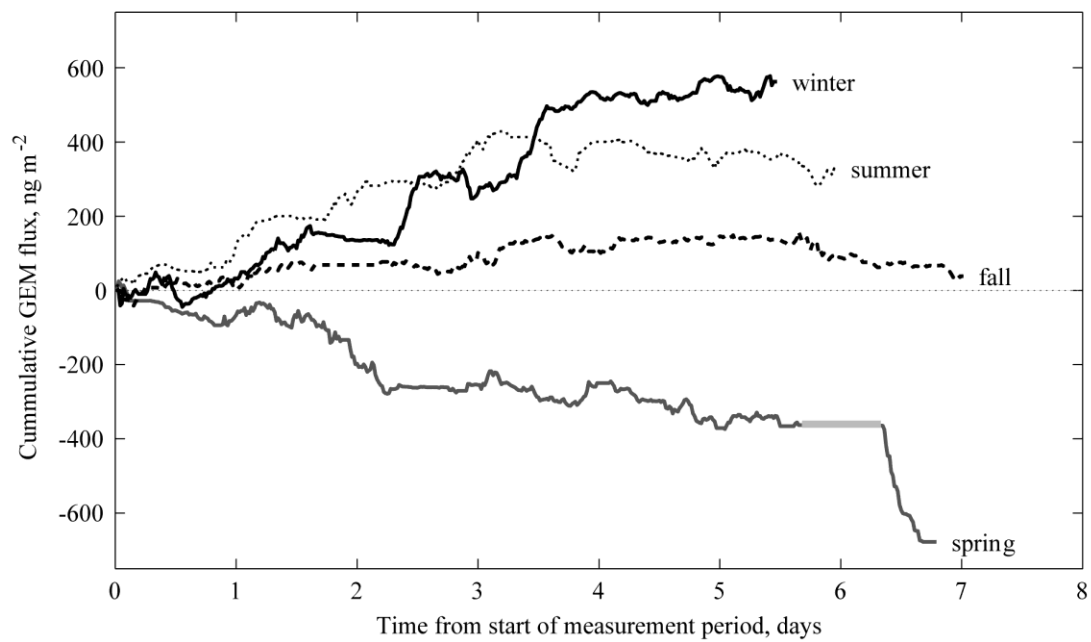


**Figure 4.** Average hourly GEM fluxes and ultraviolet (UV) radiation for each measurement period.

Error bars denote  $\pm$  one standard deviation.

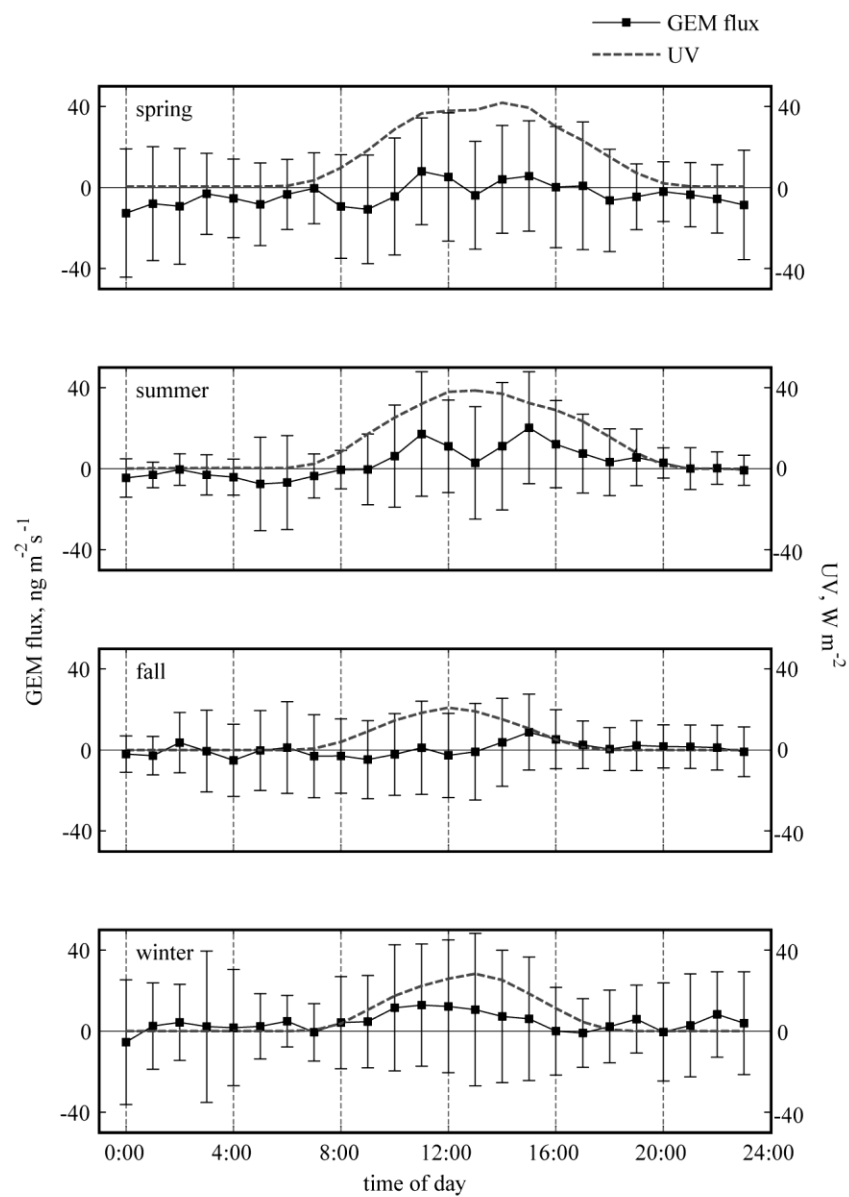


**Figure 5.** Mean *in situ* GEM fluxes from background terrestrial surfaces organized by surface type and season from a literature review. A table outlying site specific information, soil GEM concentrations, atmospheric GEM concentrations, the criteria for including/excluding studies, and the appropriate citations is provided in the supplemental information. Note that some values are mean daytime or nighttime only measurements. Soils exhibit near zero or emission fluxes across seasons. The largest deposition measurements occur over vegetated sites in the spring and summer. Gray squares indicate flux chamber measurements, and black circles indicate micrometeorological measurements.

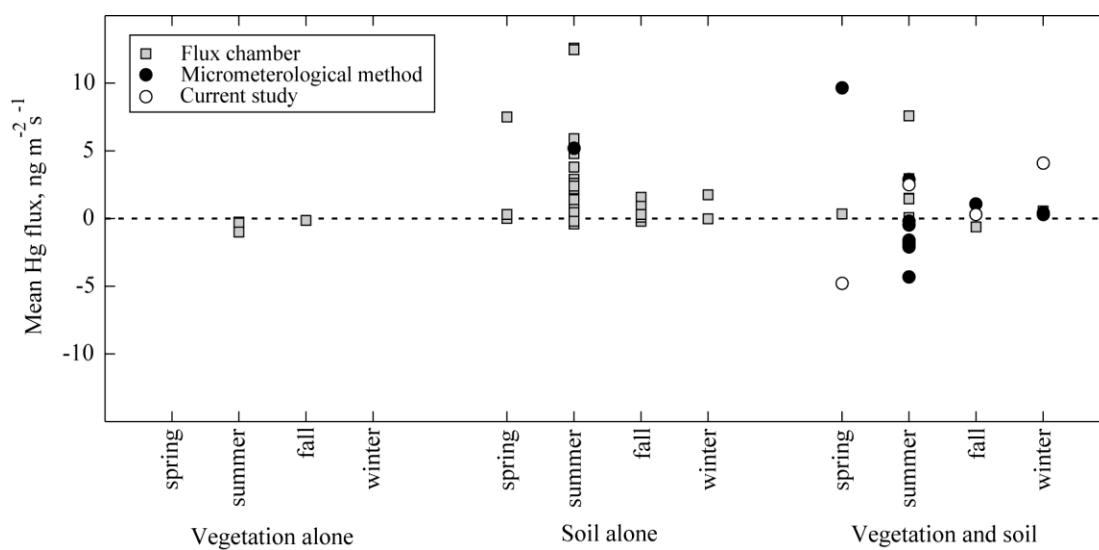


**Table 1.** Summary of micrometeorological variables, GEM concentrations and GEM fluxes for each season. †: value is not statistically different from zero ( $p>0.05$ )

| variable                                     | unit                                 | Spring<br>May 11-19, 2009 |                | Summer<br>August 6-12, 2008 |              | Fall<br>November 7-14, 2008 |                 | Winter<br>February 11-17, 2009 |                |
|--|--------------------------------------|---------------------------|----------------|-----------------------------|--------------|-----------------------------|-----------------|--------------------------------|----------------|
|  |                                      | range                     | mean           | range                       | mean         | range                       | mean            | range                          | mean           |
| Air temperature                              | °C                                   | -1.8 to 22.4              | 11.7           | 10.9 to 25.6                | 17.6         | -3.8 to 17.2                | 5.7             | -10.0 to 14.5                  | 1.3            |
| Soil temperature, 2.5 cm depth               | °C                                   | -24.1 to 29.6             | 7.9            | -1.3 to 36.2                | 14.9         | -14.84 to 22.0              | 2.5             | -23.5 to 26.5                  | 1.8            |
| Incident shortwave radiation, daytime only   | W m <sup>-2</sup> s <sup>-1</sup>    | 5.5 to 1112               | 446.7          | 5.6 to 1005                 | 435.1        | 6.3 to 682.4                | 257.1           | 5.8 to 904.8                   | 349.69         |
| UV, daytime only                             | W m <sup>-2</sup> s <sup>-1</sup>    | 0.8 to 57.1               | 23.4           | 0.4 to 55.7                 | 22.8         | 0.3 to 28.6                 | 11.9            | 0.3 to 35.2                    | 16.0           |
| PAR photon flux density, daytime only        | μmol m <sup>-2</sup> s <sup>-1</sup> | 1.7 to 269.2              | 110.7          | 2.2 to 258.7                | 115.5        | 1.9 to 172.7                | 64.7            | 1.6 to 214.2                   | 86.8           |
| g <sub>c</sub> , daytime only                | cm s <sup>-1</sup>                   | 0 to 6.5                  | 1.2            | 0 to 4.1                    | 0.8          | 0 to 5.9                    | 0.6             | 0 to 8.9                       | 0.8            |
| RH   | %                                    | 32.5 to 97.8              | 77.5           | 44.1 to 94.6                | 74.5         | 43.9 to 99.3                | 73              | 25.7 to 99.0                   | 63.6           |
| Volumetric soil moisture                     | %                                    | 48.7 to 67.1              | 55             | 32.1 to 42.8                | 40.2         | 35.3 to 47.2                | 37.1            | 25.7 to 52.2                   | 42.1           |
| Wind speed                                   | m s <sup>-1</sup>                    | 0.06 to 7.5               | 2.92           | 0.08 to 5.2                 | 2.3          | 0.36 to 5.2                 | 2.7             | 0.32 to 10.1                   | 4.2            |
| u*   | m s <sup>-1</sup>                    | 0.01 to 0.78              | 0.31           | 0.02 to 0.63                | 0.27         | 0.03 to 0.90                | 0.29            | 0.05 to 1.02                   | 0.37           |
| E (H <sub>2</sub> O flux)                    | kg m <sup>-2</sup> s <sup>-1</sup>   | -1.5 to 6.6               | 1.40           | -0.33 to 6.5                | 1.52         | -1.69 to 3.5                | 0.31            | -1.4 to 2.1                    | 0.32           |
| [CO <sub>2</sub> ]                           | mg m <sup>-3</sup>                   | 524.1 to 731.1            | 643.8          | 556.1 to 847.4              | 602.4        | 539.6 to 878.2              | 654.1           | 624.4 to 696.2                 | 666.6          |
| CO <sub>2</sub> flux                         | μmol m <sup>-2</sup> s <sup>-1</sup> | -12.7 to 16.4             | 0.11           | -12.9 to 17.0               | -0.9         | -5.6 to 8.8                 | 0.66            | -1.5 to 5.0                    | 0.18           |
| [O <sub>3</sub> ]                            | ppb                                  | 28.7 to 58.6              | 45.3           | 26.5 to 60.1                | 44.8         | 19.7 to 52.4                | 33.9            | 29.1 to 54.8                   | 41             |
| [GEM]  | ng m <sup>-3</sup>                   | 1.00 to 1.46              | 1.22           | 0.98 to 1.50                | 1.28         | 1.05 to 1.44                | 1.28            | 1.15 to 1.69                   | 1.38           |
| GEM flux, aerodynamic (± std)                | ng m <sup>-2</sup> h <sup>-1</sup>   | -125.7 to 71.0            | -4.8 (± 25.5)  | -124.8 to 82.4              | 2.5 (± 19.1) | -77.1 to 67.6               | 0.3 (± 16.8)†   | -112.0 to 119.1                | 4.1 (± 25.7)   |
| daytime                                      | ng m <sup>-2</sup> h <sup>-1</sup>   |                           | -2.1†          |                             | 6.5          |                             | 1.4†            |                                | 6.6            |
| nighttime                                    | ng m <sup>-2</sup> h <sup>-1</sup>   |                           | -7.3           |                             | -2.5         |                             | -0.4†           |                                | 2.1†           |
| GEM flux, MBR (± std)                        | ng m <sup>-2</sup> h <sup>-1</sup>   | -152.8 to 99.2            | -1.5 (± 26.6)† | -79.1 to 89.6               | 3.2 (± 21.3) | -989.6 to 870.0             | -3.0 (± 109.9)† | -770.1 to 803.6                | -2.9 (± 122.3) |
| GEM deposition velocity, aerodynamic         | cm s <sup>-1</sup>                   | -3.2 to 1.7               | -0.11          | -3.1 to 1.9                 | 0.05         | -1.9 to 1.9                 | 0.01            | -2.3 to 2.6                    | 0.09           |
| Precipitation, total for the sampling period | cm                                   | [--]                      | 6.1            | [--]                        | 0            | [--]                        | 3.9             | [--]                           | 1.1            |
| Percent energy balance closure               | %                                    | [--]                      | 70.0           | [--]                        | 79.3         | [--]                        | 82.0            | [--]                           | 78.1           |
| Percent data with winds from 30-150          | %                                    | [--]                      | 16.6           | [--]                        | 2.7          | [--]                        | 2               | [--]                           | 0.5            |
| Percent data coverage for GEM fluxes         | %                                    | [--]                      | 76.2           | [--]                        | 70.4         | [--]                        | 80.9            | [--]                           | 74.1           |

**Table 2.** Pearson correlation coefficients ( $\rho$ ) between GEM concentration, GEM fluxes (aerodynamic method), and meteorological variables. Bold font indicates a statistically significant correlation ( $p < 0.05$ ). Ozone concentrations were measured by the NPS at the Big Meadows monitoring station approximately 700 m north of the site at 1-hour intervals. Correlations were determined using averaged GEM fluxes to match the longer measurement interval.

| Variable   | Spring       |                          | Summer       |                          | Fall         |                          | Winter       |                          |
|--|--------------|--------------------------|--------------|--------------------------|--------------|--------------------------|--------------|--------------------------|
|  | [GEM]        | GEM flux,<br>aerodynamic |
| [GEM]  | [--]         | -0.07                    | [--]         | 0.09                     | [--]         | <b>-0.26</b>             | [--]         | <b>-0.14</b>             |
| GEM flux, aerodynamic                            | -0.07        | [--]                     | 0.09         | [--]                     | <b>-0.26</b> | [--]                     | <b>-0.14</b> | [--]                     |
| GEM flux, MBR                                    | <b>-0.17</b> | <b>0.62</b>              | 0.07         | <b>0.86</b>              | 0.02         | 0.03                     | -0.01        | <b>-0.24</b>             |
| Air temperature                                  | <b>0.66</b>  | <b>0.18</b>              | <b>0.67</b>  | <b>0.29</b>              | <b>-0.17</b> | -0.01                    | <b>-0.22</b> | 0.00                     |
| Soil temperature                                 | <b>0.68</b>  | <b>0.22</b>              | <b>0.55</b>  | <b>0.36</b>              | <b>-0.13</b> | 0.02                     | <b>-0.16</b> | 0.02                     |
| Incident shortwave radiation                     | <b>0.15</b>  | <b>0.19</b>              | <b>0.27</b>  | <b>0.33</b>              | -0.03        | 0.06                     | <b>-0.16</b> | <b>0.14</b>              |
| PAR  | <b>0.15</b>  | <b>0.19</b>              | <b>0.27</b>  | <b>0.33</b>              | -0.03        | 0.05                     | <b>-0.16</b> | <b>0.14</b>              |
| UV   | <b>0.17</b>  | <b>0.19</b>              | <b>0.27</b>  | <b>0.32</b>              | -0.01        | 0.04                     | <b>-0.16</b> | <b>0.14</b>              |
| Volumetric soil moisture                         | <b>-0.22</b> | -0.04                    | 0.09         | <b>-0.19</b>             | <b>0.25</b>  | -0.06                    | 0.05         | 0.00                     |
| Wind speed                                       | <b>0.44</b>  | 0.08                     | <b>0.25</b>  | <b>0.12</b>              | <b>-0.23</b> | -0.01                    | <b>-0.24</b> | -0.04                    |
| Relative humidity                                | <b>0.39</b>  | -0.03                    | <b>-0.27</b> | <b>-0.30</b>             | <b>0.27</b>  | <b>-0.14</b>             | <b>0.21</b>  | -0.07                    |
| [O <sub>3</sub> ]                                | <b>-0.27</b> | -0.07                    | <b>0.50</b>  | 0.10                     | <b>-0.41</b> | 0.04                     | <b>-0.32</b> | 0.07                     |
| [CO <sub>2</sub> ]                               | <b>-0.56</b> | <b>-0.29</b>             | <b>-0.47</b> | <b>-0.33</b>             | <b>0.37</b>  | -0.04                    | <b>0.26</b>  | 0.01                     |
| CO <sub>2</sub> flux                             | -0.04        | 0.02                     | <b>-0.22</b> | <b>-0.22</b>             | <b>-0.11</b> | <b>0.09</b>              | <b>-0.14</b> | 0.07                     |
| E (H <sub>2</sub> O flux)                        | <b>0.19</b>  | <b>0.25</b>              | <b>0.31</b>  | <b>0.32</b>              | 0.05         | 0.02                     | <b>-0.18</b> | 0.04                     |
| UV (daytime only)                                | 0.0          | <b>0.22</b>              | 0.12         | <b>0.25</b>              | <b>-0.23</b> | 0.01                     | -0.14        | <b>0.15</b>              |
| g <sub>c</sub> (H <sub>2</sub> O) (daytime only) | <b>-0.25</b> | 0.12                     | <b>-0.23</b> | -0.14                    | 0.18         | -0.10                    | <b>0.21</b>  | 0.13                     |

## Supplemental Information

### *Qualifications for inclusion in Supplementary Table 1*

Measurements were included on within Supplementary Table 1 if the site had soil Hg concentrations less than  $0.1 \mu\text{g g}^{-1}$ , a limit suggested by Gustin et al. (2000) to describe background soils. In papers with multiple sites, only those locations with concentrations lower than this limit were included. If soil Hg concentrations were not reported, they were still included if the site was described as uncontaminated by a local source and the underlying geology is thought to be low-Hg containing. Studies reporting GEM fluxes from terrestrial water bodies alone (e.g. no vegetation or soil component) were not included.

For measurements in the Northern Hemisphere, the following guidelines were used to determine the season: Spring: March 20-June 19; Summer: June 20-Sept. 19; Fall: Sept. 20 – Dec. 19; Winter: Dec. 20-March 19. The seasonal designation was chosen based on the majority of dates if the entire measurement period did not fall within one season. While it is recognized that this is somewhat of an arbitrary classification system (climatic and environmental parameters will vary on a yearly basis and depend on latitude) it provides a simple, systematic way to evaluate the diverse body of literature from a seasonal standpoint.

### *Qualifications for inclusion in Figure 5*

Measurements were included into Figure 5 only if they met the requirements listed below. Specific rational for the exclusion of a study is listed on Supplementary Table 1, with the number in parenthesis corresponding to one of the following missing criteria:

1. **Mean GEM fluxes measurements were reported.**
2. **The majority of measurements fell within a single season**, as outlined previously. Studies were not included if the site description implied that a seasonal ‘transition’ had not yet taken place.
3. **The maximum atmospheric GEM concentration was not greater than  $3.5 \text{ ng m}^{-3}$ .** If the maximum value was not reported, then the mean atmospheric GEM concentration was not greater than this limit. If no atmospheric GEM concentrations were reported, the GEM flux was still

included in the figure. This restriction was imposed to exclude ‘plume events’ and study sites where atmospheric GEM levels are substantially greater than background levels.

4. **The site did not include extensive open water.** This restriction was imposed for best comparison to the GEM fluxes reported within the current study in Shenandoah National Park, VA.

Supplementary Table 1: Approximate season, dates, site description, soil Hg concentration [ $\mu\text{g g}^{-1}$ ], atmospheric GEM concentration [ $\text{ng m}^{-3}$ ], and GEM flux [ $\text{ng m}^{-2} \text{h}^{-1}$ ] from a literature review of background terrestrial surfaces. Studies are sorted by surface type, by season, and finally by author. Studies reporting measurements across multiple seasons are listed first.

| Location   | Season | Sampling dates                    | Landcover type                           | Measurement technique | Soil Hg concentration [ $\mu\text{g g}^{-1}$ ] | Atmospheric GEM concentration [ $\text{ng m}^{-3}$ ] |       |       |      | GEM flux [ $\text{ng m}^{-2} \text{h}^{-1}$ ] |        |       |      | Notes  | Inclusion into Figure 5 | Citation             |
|--|--------|-----------------------------------|--|-----------------------|--|--|-------|-------|------|---|--------|-------|------|--------|-------------------------|----------------------|
|  |        |                                   |  |                       |  | min  | max   | mean  | std  | min   | max    | mean  | std  |        |                         |                      |
| <b>Vegetation alone</b>                                      |        |                                   |  |                       |  |  |       |       |      |   |        |       |      |        |                         |                      |
| St. Anicet, Québec, Canada                                   | Summer | July 29-31, 2004                  | Maple tree branch with 80 leaves         | FC                    | 0.063  | [-]  | [-]   | -1.02 | [-]  | [-]   | [-]    | -0.59 | [-]  | yes    | Poissant et al., 2008   |                      |
|  | Summer | Aug. 1-31, 2004                   | Maple tree branch with 80 leaves         | FC                    | 0.063  | [-]  | [-]   | -1.02 | [-]  | [-]   | [-]    | -0.51 | [-]  | yes    |                         |                      |
|  | Summer | Sept. 1-30, 2004                  | Maple tree branch with 80 leaves         | FC                    | 0.063  | [-]  | [-]   | -1.02 | [-]  | [-]   | [-]    | -0.40 | [-]  | yes    |                         |                      |
|  | Fall   | Oct. 1-22, 2004                   | Maple tree branch with 80 leaves         | FC                    | 0.063  | [-]  | [-]   | -1.02 | [-]  | [-]   | [-]    | -0.13 | [-]  | yes    |                         |                      |
| Bay St. François wetlands on Lake St. Pierre, Québec, Canada | Summer | Aug. 23-30, 2003                  | River bulrush, dry conditions            | FC                    | 0.06   | [-]  | [-]   | -1.6  | [-]  | -0.91   | 0.64   | -0.26 | 0.28 | yes    | Zhang et al., 2005      |                      |
|  | Summer | Aug. 18-22, 2003                  | River bulrush, flooded conditions        | FC                    | 0.06   | [-]  | [-]   | -1.6  | [-]  | -0.98   | 0.08   | -0.33 | 0.24 | yes    |                         |                      |
|  | Summer | Aug. 20-24, 2003                  | River bulrush, flooded conditions        | FC                    | 0.06   | 1.31   | 2.15  | 1.6   | 0.16 | -2.76   | 1.04   | -1.01 | 0.72 | yes    |                         |                      |
| Northwestern Ontario, Canada                                 | [-]    | 2001 and 2003                     | Black spruce branch, boreal ecoregion    | FC                    | [-]  | -1   | -4    | [-]   | [-]  | -24.2   | 38.5   | [-]   | [-]  | a      | no (1,2,3)              | Graydon et al., 2006 |
| Northwestern Ontario, Canada                                 | [-]    | 2001 and 2003                     | Jack pine branch, boreal ecoregion       | FC                    | [-]  | -1   | -4    | [-]   | [-]  | -19.1   | 39.8   | [-]   | [-]  | a      | no (1,2,3)              | Graydon et al., 2006 |
| <b>Soil alone</b>  |        |                                   |  |                       |  |  |       |       |      |   |        |       |      |        |                         |                      |
| Moxi platform, Sichuan province, China (A1)                  | Spring | Apr. 7-8, 2006                    | Bare agricultural soil                   | FC                    | 0.10   | 2.77   | 10.91 | 4.58  | 1.34 | 0.8   | 1118.1 | 19.2  | 28.6 | no (3) | Fu et al., 2008         |                      |
|  | Summer | Aug. 14-16, 2006                  | Agricultural soil, shaded by corn canopy | FC                    | 0.10   | 2.21   | 3.59  | 2.81  | 0.35 | 3.4   | 57.5   | 21.0  | 13.7 | no (3) |                         |                      |
|  | Winter | Dec. 13-15, 2005                  | Bare agricultural soil                   | FC                    | 0.10   | 6.28   | 9.92  | 7.17  | 0.60 | -22.5   | 17.6   | -4.1  | 5.5  | no (3) |                         |                      |
| Moxi platform, Sichuan province, China (A3)                  | Spring | Apr. 14-15, 2006                  | Bare agricultural soil                   | FC                    | 0.10   | 2.34   | 4.40  | 3.00  | 0.63 | -4.5  | 14.8   | 1.5   | 4.3  | no (3) | Fu et al., 2008         |                      |
|  | Summer | Aug. 22-25, 2006                  | Bare agricultural soil                   | FC                    | 0.10   | 2.29   | 4.45  | 3.51  | 0.44 | -3.6  | 23.3   | 2.1   | 3.9  | no (3) |                         |                      |
|  | Fall   | Sept. 30 - Oct. 2, 2006           | Bare agricultural soil                   | FC                    | 0.10   | 3.29   | 5.40  | 3.82  | 0.41 | -1.4  | 18.5   | 2.9   | 5.8  | no (3) |                         |                      |
| Tuscaloosa, Alabama  | Spring | May 28, June 10, & June 14, 2004  | Bare soil, urban                         | FC                    | [-]  | [-]  | [-]   | [-]   | [-]  | [-]   | [-]    | 7.50  | 6.10 | yes    | Gabriel et al., 2006    |                      |
|  | Summer | July 18, Sept. 4, & Sept 17, 2004 | Bare soil, urban                         | FC                    | 0.047  | [-]  | [-]   | [-]   | [-]  | [-]   | [-]    | 12.6  | 10.8 | yes    |                         |                      |
|  | Fall   | Nov. 12, Nov. 16, & Dec 3, 2004   | Bare soil, urban                         | FC                    | [-]  | [-]  | [-]   | [-]   | [-]  | [-]   | [-]    | 1.57  | 1.47 | yes    |                         |                      |
|  | Winter | Jan. 26, Feb. 10, & Feb. 18, 2004 | Bare soil, urban                         | FC                    | 0.025  | [-]  | [-]   | [-]   | [-]  | [-]   | [-]    | 1.75  | 1.35 | yes    |                         |                      |

| Location   | Season | Sampling dates             | Landcover type   | Measurement technique | Soil Hg concentration [ $\mu\text{g g}^{-1}$ ] | Atmospheric GEM concentration [ $\text{ng m}^{-3}$ ] |      |      |      | GEM flux [ $\text{ng m}^{-2} \text{h}^{-1}$ ] |       |       |      | Notes | Inclusion into Figure 5 | Citation                 |
|--|--------|----------------------------|--|-----------------------|--|--|------|------|------|---|-------|-------|------|-------|-------------------------|--------------------------|
|  |        |                            |  |                       |  | min  | max  | mean | std  | min   | max   | mean  | std  |       |                         |                          |
| Soil alone cont.   |        |                            |  |                       |  |  |      |      |      |   |       |       |      |       |                         |                          |
|  | Summer | Aug. 2005                  | Bare soil  | FC                    | <0.05  | [-]  | [-]  | 2.9  | 3.8  | [-]   | [-]   | 0.5   | 0.6  |       | no (3)                  |                          |
| NW of Elko, Nevada (NV99)                                      | Fall   | Oct. 2005                  | Bare soil  | FC                    | <0.05  | [-]  | [-]  | 2.0  | 0.8  | [-]   | [-]   | -0.2  | 0.3  |       | yes                     | Gustin et al., 2006      |
|  | Winter | March 2005                 | Bare soil  | FC                    | <0.05  | [-]  | [-]  | 2.2  | 0.7  | [-]   | [-]   | -0.02 | 0.6  |       | yes                     |                          |
| Standing Stone State Forest, Tennessee                         | Spring | Apr. 2004 - June 2004      | Forest floor, maple and hardwood canopy                | FC                    | 0.023 to 0.092                                 | 1.3  | 3.3  | 1.7  | 0.4  | -1.2  | 1.2   | 0.0   | 0.3  | a     | yes                     | Kuiken et al., 2008a     |
|  | Summer | July 2004 - Sept. 2004     | Forest floor, maple and hardwood canopy                | FC                    | 0.023 to 0.092                                 | 0.9  | 2.4  | 1.3  | 0.2  | -0.1  | 1.0   | 0.4   | 0.3  | a     | yes                     |                          |
|  | Fall   | Oct. 2004 - Nov. 2004      | Forest floor, maple and hardwood canopy (little shade) | FC                    | 0.023 to 0.092                                 | 1.3  | 1.9  | 1.6  | 0.2  | 0.0   | 2.9   | 0.9   | 0.6  | a     | yes                     |                          |
|  | Winter | Jan. 2004 - March 2004     | Forest floor, maple and hardwood canopy (little shade) | FC                    | 0.023 to 0.092                                 | 1.7  | 4.8  | 2.4  | 0.8  | -0.4  | 3.3   | 0.6   | 0.5  | a     | no (3)                  |                          |
| Near Lake Gårdsjön, Sweden                                     | Spring | May & June 1988-9          | Forest floor, organic layer, conifer canopy            | FC                    | [-]  | 2.38   | 2.79 | [-]  | [-]  | -1.0  | 2.5   | 0.3   | 0.4  | c     | yes                     | Xiao et al., 1991        |
|  | Winter | Feb., April, & Dec. 1987-8 | Forest floor, organic layer, conifer canopy            | FC                    | [-]  | 2.06   | 3.72 | [-]  | [-]  | -2.0  | 1.4   | -0.9  | 0.4  | a, c  | no (3)                  |                          |
| Six forested sites on the eastern seaboard, United States      | Spring | May-June 2005              | Forest floor, evergreen and deciduous canopy           | FC                    | 0.013 to 0.219                                 | 1.1  | 13.2 | [-]  | [-]  | -5.1  | 2.5   | 0.2   | 0.9  | a     | no (1)                  | Kuiken et al., 2008b     |
| Lake Gårdsjön, Sweden  | Spring | June 2-10, 1994            | Forest floor with moss, decaying needles and shrubs    | MM                    | [-]  | 1.48   | 2.68 | [-]  | [-]  | -5.4  | 4.2   | [-]   | [-]  | a, g  | no (1)                  | Lindberg et al., 1998    |
| Nevada (n=22)  | Spring | April 28 - June 15, 2000   | Bare soil  | FC                    | 0.01 to 0.062                                  | [-]  | [-]  | [-]  | [-]  | -3.47   | 17.09 | [-]   | [-]  | a     | no (2)                  | Nacht and Gustin, 2004   |
| Walker Branch Watershed, Oak Ridge, Tennessee (Nelson)         | Summer | Apr. - Aug. 1995           | Field, grass removed                                   | FC                    | 0.061  | [-]  | [-]  | [-]  | [-]  | -1.81   | 18.70 | 12.47 | 5.44 | a     | yes                     | Carpi and Lindberg, 1998 |
| Rouyn-Noranda, Quebec  | Summer | July 24 - Aug. 3, 2000     | Sand and gravel pit                                    | MM                    | 0.010  | [-]  | [-]  | [-]  | [-]  | [-]   | [-]   | 5.2   | 0.07 | f     | yes                     | Edwards et al., 2005     |
| Mohave Desert, California (D1, n=4)                            | Summer | July 2003                  | Desert soils   | FC                    | 0.012 to 0.032                                 | 0.7  | 2.0  | 1.4  | 0.02 | 0.0   | 2.7   | 0.6   | 0.07 |       | yes                     | Ericksen et al., 2006    |
| Black Kettle Grasslands Preserve, Cheyenne, Oklahoma (G3, n=4) | Summer | July - Aug. 2003           | Grassland soils  | FC                    | <0.010 to 0.010                                | 0.5  | 1.5  | 0.8  | 0.01 | 0.1   | 3.5   | 1.0   | 0.06 |       | yes                     | Ericksen et al., 2006    |
| Wichita Mountains, Oklahoma (G2, n=4)                          | Summer | July - Aug. 2003           | Grassland soils  | FC                    | 0.011 to 0.020                                 | 0.6  | 1.3  | 0.8  | 0.01 | -0.1  | 3.4   | 1.4   | 0.09 |       | yes                     | Ericksen et al., 2006    |
| Central Oklahoma prairie (G1, n=4)                             | Summer | July - Aug. 2003           | Grassland soils  | FC                    | <0.010 to 0.022                                | 0.5  | 3.2  | 1.1  | 0.01 | 0.3   | 9.7   | 2.5   | 0.14 |       | yes                     | Ericksen et al., 2006    |
| Cherokee National Grasslands, Colorado (G4, n=4)               | Summer | July - Aug. 2003           | Grassland soils  | FC                    | <0.010 to 0.019                                | 0.3  | 0.5  | 0.4  | 0.01 | 0.2   | 1.1   | 0.5   | 0.05 | a     | yes                     | Ericksen et al., 2006    |
| Hailuoguo valley, Sichuan province, China (F6)                 | Summer | Aug. 31 - Sept. 1, 2006    | Forest floor, pine forest canopy                       | FC                    | 0.08   | 0  | 2.66 | 1.60 | 0.58 | -0.6  | 10.6  | 2.9   | 2.0  |       | yes                     | Fu et al., 2008          |
| Caoko valley, Cichuan province, China (F2)                     | Summer | Aug. 27-29, 2006           | Forest floor, defoliated broadleaf canopy              | FC                    | 0.06   | 2.58   | 4.68 | 3.70 | 0.50 | 0.05  | 21.1  | 5.7   | 4.7  |       | no (3)                  | Fu et al., 2008          |

| Location   | Season | Sampling dates        | Landcover type  | Measurement technique | Soil Hg concentration [ $\mu\text{g g}^{-1}$ ] | Atmospheric GEM concentration [ $\text{ng m}^{-3}$ ] |      |      |      | GEM flux [ $\text{ng m}^{-2} \text{h}^{-1}$ ] |       |      |      | Notes | Inclusion into Figure 5 | Citation               |
|--|--------|-----------------------|---|-----------------------|--|--|------|------|------|---|-------|------|------|-------|-------------------------|------------------------|
|  |        |                       |   |                       |  | min  | max  | mean | std  | min   | max   | mean | std  |       |                         |                        |
| <b>Soil alone cont.</b>                              |        |                       |   |                       |  |  |      |      |      |   |       |      |      |       |                         |                        |
| Yanzigou valley, Sichuan province, China (F1)        | Summer | Aug. 21-22, 2006      | Forest floor, organic layer, shrub canopy                   | FC                    | 0.09   | 2.36   | 8.54 | 3.58 | 1.26 | 1.4   | 20.7  | 6.6  | 4.2  |       | no (3)                  | Fu et al., 2008        |
| Near Dadu River, Sichuan province, China (A5)        | Summer | Sept. 4-6, 2006       | Bare agricultural soil                                      | FC                    | 0.08   | 2.09   | 4.85 | 3.35 | 0.50 | 0.8   | 142.0 | 24.5 | 38.3 |       | no (3)                  | Fu et al., 2008        |
| Negro River Basin, Amazon (CARV-1)                   | Summer | Jan. 20-22, 2003      | Forest floor, tropical forest canopy                        | FC                    | 0.084  | 0.5  | 1.6  | 0.9  | 0.5  | [-]   | [-]   | 0.2  | 0.2  | a     | yes                     | Magarelli et al., 2005 |
|  |        |                       |   |                       |  |  |      |      |      |   |       | -0.4 | 0.2  | b     | yes                     |                        |
| Negro River Basin, Amazon (CARV-2/03)                | Summer | Jan. 23-25, 2003      | open field, slash and burn agriculture                      | FC                    | 0.071  | 0.3  | 2.7  | 0.9  | 0.1  | [-]   | [-]   | 4.8  | 0.6  | a     | yes                     | Magarelli et al., 2005 |
|  |        |                       |   |                       |  |  |      |      |      |   |       | 2.6  | 1    | b     | yes                     |                        |
| Negro River Basin, Amazon (CARV-2/04)                | Summer | Jan. 17-18, 2004      | open field, slash and burn agriculture                      | FC                    | 0.071  | 0.2  | 0.5  | 0.3  | 0.1  | [-]   | [-]   | 3.8  | 3.2  | a     | yes                     | Magarelli et al., 2005 |
|  |        |                       |   |                       |  |  |      |      |      |   |       | 0.1  | 0.2  | b     | yes                     |                        |
| Negro River Basin, Amazon (BAR)                      | Summer | Jan. 21-23, 2004      | open field, agricultural                                    | FC                    | 0.106  | 0.2  | 0.3  | 0.3  | 0.1  | [-]   | [-]   | 2    | 0.2  | a     | yes                     | Magarelli et al., 2005 |
|  |        |                       |   |                       |  |  |      |      |      |   |       | 0.6  | 0.2  | b     | yes                     |                        |
| Nevada (n=26)  | Summer | July 2 - Aug. 4, 2000 | Bare soil   | FC                    | 0.01 to 0.064                                  | [-]  | [-]  | [-]  | [-]  | -15.4   | 41.7  | [-]  | [-]  | a     | no (1)                  | Nacht and Gustin, 2004 |
| Bay St. François wetlands on Lake St. Pierre, Canada | Summer | Aug. - Sept. 1999     | Dry wetland, bare soil with vegetation removed              | FC                    | 0.06   | 0.56   | 5.65 | [-]  | [-]  | -1.5  | 2.4   | [-]  | [-]  |       | no (1)                  | Poissant et al., 2004a |
| Gothenburg, Sweden                                   | Summer | Aug. 4-11, 1987       | Conifer forest floor, deciduous forest floor and open field | FC                    | [-]  | [-]  | [-]  | [-]  | [-]  | 0.1   | 1.4   | 1.1  | 0.4  | a, c  | yes                     | Schroeder et al., 1989 |
| Kuujuarapik, Quebec                                  | Summer | Aug. 2001             | Sand  | FC                    | [-]  | [-]  | [-]  | [-]  | [-]  | [-]   | [-]   | 0.44 | [-]  |       | yes                     | Schroeder et al., 2005 |
| Rouyn Noranda, Quebec                                | Summer | July - Aug. 2000      | Sand and gravel pit   | FC                    | 0.01   | [-]  | [-]  | [-]  | [-]  | [-]   | [-]   | 5.9  | [-]  |       | yes                     | Schroeder et al., 2005 |
| <b>Vegetation and soil</b>                           |        |                       |   |                       |  |  |      |      |      |   |       |      |      |       |                         |                        |
| Ontario, Quebec and Nova Scotia                      | Summer | summers of 1997-2000  | Rock/till   | FC                    | 0.005 to 0.25                                  | [-]  | [-]  | [-]  | [-]  | -0.03   | 1.7   | [-]  | [-]  |       | no (1)                  | Schroeder et al., 2005 |
| Upper Peninsula, Michigan (Upper Falls)              | Summer | June 24, 1998         | Forest floor, hardwood canopy                               | FC                    | <0.1   | 1.2  | 1.4  | 1.3  | 0.06 | -0.6  | 0.6   | -0.2 | 0.3  | a     | yes                     | Zhang et al., 2001     |
| Upper Peninsula, Michigan (Taq. River Mouth)         | Summer | June 26, 1998         | Forest floor, mixed forest canopy                           | FC                    | <0.1   | 1.3  | 1.6  | 1.4  | 0.09 | 1.1   | 1.7   | 1.4  | 0.3  | a     | yes                     | Zhang et al., 2001     |
| Upper Peninsula, Michigan (Hardwood)                 | Summer | June 19, 1998         | Forest floor, hardwood canopy                               | FC                    | 0.069  | 2.1  | 2.2  | 2.1  | 0.08 | 0.6   | 3.7   | 2.2  | 0.9  | a     | yes                     | Zhang et al., 2001     |
| Upper Peninsula, Michigan (Pine)                     | Summer | June 21, 1998         | Forest floor, pine canopy                                   | FC                    | 0.006 to 0.098                                 | 2.0  | 2.9  | 2.4  | 0.30 | 1.7   | 3.5   | 2.4  | 1.0  | a     | yes                     | Zhang et al., 2001     |

| Location   | Season               | Sampling dates                                | Landcover type  | Measurement technique | Soil Hg concentration [ $\mu\text{g g}^{-1}$ ] | Atmospheric GEM concentration [ $\text{ng m}^{-3}$ ] |       |       |      | GEM flux [ $\text{ng m}^{-2} \text{h}^{-1}$ ] |       |       |      | Notes | Inclusion into Figure 5 | Citation                           |
|--|----------------------|---|---|-----------------------|--|--|-------|-------|------|---|-------|-------|------|-------|-------------------------|------------------------------------|
|  |                      |   |   |                       |  | min  | max   | mean  | std  | min   | max   | mean  | std  |       |                         |                                    |
| <b>Vegetation and soil cont.</b>                           |                      |   |   |                       |  |  |       |       |      |   |       |       |      |       |                         |                                    |
| North Dakota (G6, n=3)                                     | Fall                 | Oct. 2003                                     | Grassland, soils  | FC                    | 0.042 to 0.055                                 | 1.5  | 2.0   | 1.8   | 0.05 | -0.2  | 0.8   | 0.1   | 0.09 | a     | yes                     | Ericksen et al., 2006              |
| Wisconsin (G5, n=9)  | Fall                 | Sept. 2003                                    | Grassland, soils  | FC                    | <0.010 to 0.028                                | 0.7  | 3.2   | 1.3   | 0.02 | -0.9  | 3.5   | 0.3   | 0.07 |       | yes                     | Ericksen et al., 2006              |
| Hungry Valley, Nevada (D2, n=5)                            | Monthly measurements | May 2003 - May 2004                           | Desert, sparse vegetation   | FC                    | 0.030  | 0.2  | 4.0   | 1.3   | 0.01 | -1.5  | 4.2   | 0.2   | 0.03 |       | no (2, 3)               | Ericksen et al., 2006              |
| Yellowstone National Park (PF)                             | [-]                  | [-]   | Forest floor, thick organic layer, pine canopy                              | FC                    | 0.040  | 0.7  | 1.4   | 1.0   | 0.01 | -0.3  | 3.7   | 0.3   | 0.10 |       | no (2)                  | Ericksen et al., 2006              |
| Foothills of Sierra Nevada Mountains, California (MF, n=4) | [-]                  | [-]   | Forest floor, organic layer, mixed forest canopy                            | FC                    | 0.032 to 0.060                                 | 1.0  | 2.3   | 1.4   | 0.02 | -0.2  | 3.8   | 1.1   | 0.10 |       | no (2)                  | Ericksen et al., 2006              |
| Underwood, North Dakota (A, n=4)                           | [-]                  | [-]   | Argicultural soils, organic layer   | FC                    | 0.029 to 0.035                                 | 1.4  | 3.7   | 2.3   | 0.08 | -1.4  | 5.0   | 1.2   | 0.52 | a     | no (2, 3)               | Ericksen et al., 2006              |
| Shenandoah National Park, Virginia                         | Spring               | May 11-19, 2009                               | Grassland/wetland, emerging vegetation                                      | MM                    | 0.10   | 1.00   | 1.46  | 1.22  | 0.09 | -125.7  | 71.0  | -4.8  | 25.5 | f     | yes                     | Current study                      |
|  | Summer               | Aug. 6-12, 2008                               | Grassland/wetland, after full leaf out                                      | MM                    | 0.10   | 0.98   | 1.50  | 1.28  | 0.07 | -124.8  | 82.4  | 2.5   | 19.1 | f     | yes                     |                                    |
|  | Fall                 | Nov. 7-14, 2008                               | Grassland/wetland, undergoing senescence                                    | MM                    | 0.10   | 1.05   | 1.44  | 1.28  | 0.07 | -90.1   | 81.8  | 0.3   | 19.8 | f     | yes                     |                                    |
|  | Winter               | Feb. 11-17, 2009                              | Grassland/wetland, dead canopy  | MM                    | 0.10   | 1.15   | 1.69  | 1.38  | 0.08 | -112.0  | 119.1 | 4.1   | 25.7 | f     | yes                     |                                    |
| Fruebel, Switzerland                                       | Summer               | Aug. 26-Nov. 23, 2005 & Mar. 27-Aug. 30, 2006 | Grassland used for hay production and cattle grazing (vegetation present)   | MM                    | 0.10   | -0.69  | -2.42 | -1.42 | [-]  | -42   | 20    | -4.3  | [-]  | f, †  | yes                     | Fritsche et al., 2008a             |
|  |                      |   |   |                       |  |  |       |       |      | -35   | 34    | -1.7  | [-]  | g, †  | yes                     |                                    |
|  | Winter               | Nov. 24, 2005 - Mar. 26, 2006                 | Grassland used for hay production and cattle grazing (snow covered surface) | MM                    | 0.10   | -0.69  | -2.42 | -1.42 | [-]  | -34   | 29    | 0.3   | [-]  | f, †  | yes                     |                                    |
| Tuscaloosa, Alabama  | Spring               | May 26, June 2, & June 12, 2004               | Grass, urban  | FC                    | [-]  | [-]  | [-]   | [-]   | [-]  | [-]   | [-]   | 0.34  | 1.03 |       | yes                     | Gabriel et al., 2006               |
|  | Summer               | July 17, Aug. 29, & Sept 5, 2004              | Grass, urban  | FC                    | 0.034  | [-]  | [-]   | [-]   | [-]  | [-]   | [-]   | 1.45  | 1.62 |       | yes                     |                                    |
|  | Fall                 | Nov. 13, Nov. 17, & Dec 4, 2004               | Grass, urban  | FC                    | [-]  | [-]  | [-]   | [-]   | [-]  | [-]   | [-]   | -0.62 | 0.54 |       | yes                     |                                    |
|  | Winter               | Jan. 30, Feb. 17, & Feb. 21, 2004             | Grass, urban  | FC                    | 0.035  | [-]  | [-]   | [-]   | [-]  | [-]   | [-]   | 0.55  | 1.00 |       | yes                     |                                    |
| Near St. Paul, Minnesota                                   | Spring               | May 7-14 & May 31 - June 8, 2001              | Argicultural field, freshly planted corn, mostly bare soil                  | MM                    | 0.0248   | 1.23   | 2.65  | 1.47  | [-]  | -91.7   | 190.5 | 9.67  | [-]  |       | yes                     | Cobos et al., 2002                 |
| Kang Hwa Island, Korea                                     | Spring               | Mar. 20-27, 2001                              | Rice paddy field, dry with rice seedings                                    | MM                    | [-]  | 2.21   | 8.35  | 3.72  | 1.10 | -136  | 1071  | 183   | 236  |       | no (3)                  | Kim et al., 2002; Kim et al., 2003 |
| Kang Hwa Island, Korea                                     | Spring               | Apr. 23-30, 2002                              | Rice paddy field, dry with rice seedings                                    | MM                    | [-]  | 1.30   | 6.25  | 2.57  | 0.91 | -112  | 454   | 27.9  | 97.4 |       | no (3)                  | Kim et al., 2003                   |

| Location                                      | Season | Sampling dates          | Landcover type   | Measurement technique | Soil Hg concentration [ $\mu\text{g g}^{-1}$ ] | Atmospheric GEM concentration [ $\text{ng m}^{-3}$ ] |      |       |       | GEM flux [ $\text{ng m}^{-2} \text{h}^{-1}$ ] |       |       |      | Notes | Inclusion into Figure 5 | Citation  |
|---|--------|-------------------------|--|-----------------------|--|--|------|-------|-------|---|-------|-------|------|-------|-------------------------|---|
|   |        |                         |  |                       |  | min  | max  | mean  | std   | min   | max   | mean  | std  |       |                         |   |
| <b>Vegetation and soil cont.</b>              |        |                         |  |                       |  |  |      |       |       |   |       |       |      |       |                         |   |
| Walker Branch Watershed, Oak Ridge, Tennessee | Summer | July 15 - Sept 21, 1993 | Above the canopy of an uneven aged oak hickory forest  | MM                    | [-]  | 1.41   | 3.82 | [-]   | [-]   | -230  | 290   | [-]   | [-]  | a, g  | no (1, 3)               | Lindberg et al., 1998                               |
| Fruebel, Switzerland                          | Summer | June 7 - July 20, 2006  | Grassland used for cattle grazing                      | MM                    | 0.10   | 0.76   | 1.61 | 1.20  | [-]   | -27   | 14    | -4.3  | [-]  | f, †  | yes                     | Fritsche et al., 2008b                              |
|   |        |                         |  |                       |  |  |      |       |       | -14   | 14    | -1.6  | [-]  | g, †  | yes                     |   |
| Neustift, Austria                             | Summer | June 14 - 29, 2006      | Grassland used for hay production, intensively managed | MM                    | 0.044  | 0.48   | 1.70 | 1.22  | [-]   | -41   | 26    | -2.1  | [-]  | f, †  | yes                     | Fritsche et al., 2008b                              |
|   |        |                         |  |                       |  |  |      |       |       | -76   | 37    | -0.5  | [-]  | g, †  | yes                     |   |
| Oensingen, Switzerland                        | Summer | Sept. 14 - 26, 2006     | Experimental farmland, intensively managed             | MM                    | 0.071  | 0.94   | 4.71 | 1.66  | [-]   | -33   | 29    | 0.2   | [-]  | f, †  | no (3)                  | Fritsche et al., 2008b                              |
|   |        |                         |  |                       |  |  |      |       |       | -18   | 30    | 0.3   | [-]  | g, †  | no (3)                  |   |
| Seebodenalp, Switzerland                      | Summer | June - July, 2004       | Subalpine grassland, extensively grazed                | MM                    | [-]  | [-]  | [-]  | 1.654 | 0.005 | -0.9  | 1.8   | -0.2  | 0.3  | b, h  | yes                     | Obrist et al., 2006                                 |
|   |        |                         |  |                       |  |  |      |       |       | [-]   | [-]   | -1.92 | 0.22 | g     | yes                     |   |
| Saint-Anicet, Quebec, Canada                  | Summer | July 21-23, 1995        | Grassy, rural pasture                                  | FC                    | 0.006  | 1.53   | 5.12 | 2.50  | 0.63  | 0.62  | 8.29  | 2.95  | 2.15 | e     | yes                     | Poissant and Casimir., 1998; Schroeder et al., 2005 |
| Thunder Bay, Ontario, Canada                  | Summer | June 2000               | Fallow field, overburden Hg-rich geology               | MM                    | 0.1  | [-]  | [-]  | [-]   | [-]   | [-]   | [-]   | 2.9   | [-]  |       | yes                     | Schroeder et al., 2005                              |
| Kuujuarapikm Quebec, Canada                   | Summer | Aug. 2001               | Moss   | FC                    | [-]  | [-]  | [-]  | [-]   | [-]   | -0.58   | 1.3   | 0.08  | [-]  |       | yes                     | Schroeder et al., 2005                              |
| MacMillan Pass, Yukon Territory, Canada       | Summer | July 2001               | Moss, overburden Hg-rich geology                       | FC                    | [-]  | [-]  | [-]  | [-]   | [-]   | -0.60   | 10.63 | 1.5   | [-]  |       | yes                     | Schroeder et al., 2005                              |
| Tahquamenon River watershed, Michigan         | Summer | June 20, 1998           | Open grassy field                                      | FC                    | 0.016  | 1.8  | 3.1  | 2.4   | 0.40  | 5.0   | 10.2  | 7.6   | 1.7  | a     | yes                     | Zhang et al., 2001                                  |
| Hopetown, Ontario, Canada                     | Fall   | Sept. 18-24, 1999       | Pasture, overburden Hg-rich geology                    | MM                    | 0.047  | [-]  | [-]  | [-]   | [-]   | [-]   | [-]   | 1.1   | [-]  | f     | yes                     | Edwards et al., 2005; Schroeder et al., 2005        |
| Wartburg, Tennessee                           | Fall   | Sept. 27 - Oct. 6, 1994 | Above the canopy of a pine tree plantation             | MM                    | 0.05   | 1.19   | 1.67 | [-]   | [-]   | -33   | 86    | [-]   | [-]  | a, g  | no (1)                  | Lindberg et al., 1998                               |
| Moxi platform, Sichuan province, China (A2)   | Winter | Dec. 12-13, 2005        | Agricultural soil with wheat seedlings                 | FC                    | 0.10   | 3.75   | 7.39 | 5.10  | 0.92  | -10.2   | 11.4  | -3.1  | 4.7  |       | no (3)                  | Fu et al., 2008                                     |

| Location   | Season | Sampling dates          | Landcover type                                 | Measurement technique | Soil Hg concentration [ $\mu\text{g g}^{-1}$ ] | Atmospheric GEM concentration [ $\text{ng m}^{-3}$ ] |      |      |      | GEM flux [ $\text{ng m}^{-2} \text{h}^{-1}$ ] |      |      |      | Notes | Inclusion into Figure 5 | Citation               |
|--|--------|-------------------------|--|-----------------------|--|--|------|------|------|---|------|------|------|-------|-------------------------|------------------------|
|  |        |                         |  |                       |  | min  | max  | mean | std  | min   | max  | mean | std  |       |                         |                        |
| <b>Vegetation, soil, and water</b>                                   |        |                         |  |                       |  |  |      |      |      |   |      |      |      |       |                         |                        |
| Between the Florida Everglades and Lake Okeechobee agricultural area | Spring | Apr. 11-12, 1996        | Managed wetlands, open water and vegetation    | MM                    | [-]  | [-]  | [-]  | [-]  | [-]  | [-]   | [-]  | 38.0 | 68   | a, g  | no (4)                  | Lindberg et al., 2002  |
|  | Summer | June 15 - July 9, 1997  | Managed wetlands, open water and vegetation    | MM                    | [-]  | [-]  | [-]  | [-]  | [-]  | [-]   | [-]  | 37.0 | 49   | a, g  | no (4)                  |                        |
|  | Fall   | Nov. 9-11, 1997         | Managed wetlands, open water and vegetation    | MM                    | [-]  | [-]  | [-]  | [-]  | [-]  | [-]   | [-]  | 42.0 | 50   | a, g  | no (4)                  |                        |
|  | Winter | Mar. 4-18, 1997         | Managed wetlands, open water and vegetation    | MM                    | [-]  | [-]  | [-]  | [-]  | [-]  | [-]   | [-]  | 16.9 | 23   | a, g  | no (4)                  |                        |
| Lake Saint-Pierre, Quebec, Canada                                    | Spring | May 2000                | Marsh, wet conditions, sediment not exposed    | MM                    | [-]  | [-]  | [-]  | [-]  | [-]  | -0.46   | 7.13 | 0.95 | [-]  |       | no (4)                  | Schroeder et al., 2005 |
|  | Summer | July-Aug. 1999          | Marsh, dry conditions, sediment exposed        | MM                    | 0.011  | [-]  | [-]  | [-]  | [-]  | -1.5  | 2.40 | 0.88 | [-]  |       | no (4)                  |                        |
| Florida Everglades   | Spring | June 5-21, 2000         | Sawgrass and cattail marshes, wetland prairies | MM                    | [-]  | [-]  | [-]  | [-]  | [-]  | [-]   | [-]  | 16   | 30   | a, g  | no (4)                  | Marsik et al., 2005    |
|  |        |                         |  |                       |  |  |      |      |      | [-]   | [-]  | -1   | 4    | b, g  | no (4)                  |                        |
| Bay St. François wetlands on Lake St. Pierre, Canada                 | Summer | Aug. 23 - Sept. 3, 2002 | Wetlands, open water and mixed vegetation      | MM                    | 0.06   | 0.85   | 2.16 | 1.38 | 1.18 | -110  | 278  | 32.1 | 55.6 | g     | no (4)                  | Poissant et al., 2004b |

a: daytime values only  
 b: nighttime values only  
 c: chamber blocks light  
 d: plants uprooted  
 e: only recorded evasion  
 f: Aerodynamic method  
 g: Modified Bowen Ratio method  
 h: Rn222/Hg method  
 †: Data incorporates an averaging technique  
 MM: Micrometeorological method  
 FC: Flux chamber

**REFERENCES: CHAPTER 2**

- Bahlmann, E., R. Ebinghaus, and W. Ruck (2006), Development and application of a laboratory flux measurement system (LFMS) for the investigation of the kinetics of mercury emissions from soils, *Journal of Environmental Management*, 81(2), 114-125.
- Baldocchi, D. D., B. B. Hicks, and T. P. Meyers (1988), Measuring biosphere-atmosphere exchanges of biologically related gases with micrometeorological methods, *Ecology*, 69(5), 1331-1340.
- Browne, C. L., and S. C. Fang (1978), Uptake of mercury vapor by wheat: an assimilation model, *Plant Physiology*, 61(3), 430-433.
- Brutsaert, W. (1982), *Evaporation into the atmosphere : theory, history, and applications*, x, 299 p. pp., Reidel ;Sold and distributed in the U.S.A. and Canada by Kluwer Boston, Dordrecht, Holland; Boston Hingham, MA.
- Buchholz, A. (2006), Characterization of the diffusion of non-electrolytes across plant cuticles: properties of the lipophilic pathway, *Journal of Experimental Botany*, 57, 2501-2513
- Bushey, J. T., A. G. Nallana, M. R. Montesdeoca, and C. T. Driscoll (2008), Mercury dynamics of a northern hardwood canopy, *Atmospheric Environment*, 42(29), 6905-6914.
- Carpi, A., and S. E. Lindberg (1997), Sunlight-mediated emission of elemental mercury from soil amended with municipal sewage sludge, *Environmental Science & Technology*, 31(7), 2085-2091.
- Carpi, A., and S. E. Lindberg (1998), Application of a Teflon (TM) dynamic flux chamber for quantifying soil mercury flux: Tests and results over background soil, *Atmospheric Environment*, 32(5), 873-882.
- Cobos, D. R., J. M. Baker, and E. A. Nater (2002), Conditional sampling for measuring mercury vapor fluxes, *Atmospheric Environment*, 36(27), 4309-4321.
- Ebinghaus, R., H. H. Kock, A. M. Coggins, T. G. Spain, S. G. Jennings, and C. Temme (2002), Long-term measurements of atmospheric mercury at Mace Head, Irish west coast, between 1995 and 2001, *Atmospheric Environment*, 36(34), 5267-5276.

- Edwards, G. C., P. E. Rasmussen, W. H. Schroeder, D. M. Wallace, L. Halfpenny-Mitchell, G. M. Dias, R. J. Kemp, and S. Ausma (2005), Development and evaluation of a sampling system to determine gaseous Mercury fluxes using an aerodynamic micrometeorological gradient method, *Journal of Geophysical Research-Atmospheres*, 110(D10).
- Engle, M. A., M. S. Gustin, and H. Zhang (2001), Quantifying natural source mercury emissions from the Ivanhoe Mining District, north-central Nevada, USA, *Atmospheric Environment*, 35(23), 3987-3997.
- Engle, M. A., M. S. Gustin, S. E. Lindberg, A. W. Gertler, and P. A. Ariya (2005), The influence of ozone on atmospheric emissions of gaseous elemental mercury and reactive gaseous mercury from substrates, *Atmospheric Environment*, 39(39), 7506-7517.
- Ericksen, J. A., M. S. Gustin, M. Xin, P. J. Weisberg, and G. C. J. Fernandez (2006), Air-soil exchange of mercury from background soils in the United States, *Science of the Total Environment*, 366(2-3), 851-863.
- Ericksen, J. A., M. S. Gustin, D. E. Schorran, D. W. Johnson, S. E. Lindberg, and J. S. Coleman (2003), Accumulation of atmospheric mercury in forest foliage, *Atmospheric Environment*, 37(12), 1613-1622.
- Fay, L., and M. Gustin (2007), Assessing the influence of different atmospheric and soil mercury concentrations on foliar mercury concentrations in a controlled environment, *Water Air and Soil Pollution*, 181(1-4), 373-384.
- Frescholtz, T. F., M. S. Gustin, D. E. Schorran, and G. C. J. Fernandez (2003), Assessing the source of mercury in foliar tissue of quaking aspen, *Environmental Toxicology and Chemistry*, 22(9), 2114-2119.
- Fritsche, J., D. Obrist, M. J. Zeeman, F. Conen, W. Eugster, and C. Alewell (2008a), Elemental mercury fluxes over a sub-alpine grassland determined with two micrometeorological methods, *Atmospheric Environment*, 42(13), 2922-2933.

- Fritsche, J., G. Wohlfahrt, C. Ammann, M. Zeeman, A. Hammerle, D. Obrist, and C. Alewell (2008b),  
Summertime elemental mercury exchange of temperate grasslands on an ecosystem-scale,  
*Atmospheric Chemistry and Physics*, 8(24), 7709-7722.
- Fu, X. W., X. B. Feng, and S. F. Wang (2008), Exchange fluxes of Hg between surfaces and  
atmosphere in the eastern flank of Mount Gongga, Sichuan province, southwestern China,  
*Journal of Geophysical Research-Atmospheres*, 113(D20).
- Gabriel, M. C., D. G. Williamson, H. Zhang, S. Brooks, and S. Lindberg (2006), Diurnal and seasonal  
trends in total gaseous mercury flux from three urban ground surfaces, *Atmospheric  
Environment*, 40(23), 4269-4284.
- Graydon, J. A., V. L. St Louis, S. E. Lindberg, H. Hintelmann, and D. P. Krabbenhoft (2006),  
Investigation of mercury exchange between forest canopy vegetation and the atmosphere  
using a new dynamic chamber, *Environmental Science & Technology*, 40(15), 4680-4688.
- Grigal, D. F. (2002), Inputs and outputs of mercury from terrestrial watersheds: a review,  
*Environmental Reviews*, 10, 1-39.
- Gustin, M. S., G. E. Taylor, and R. A. Maxey (1997), Effect of temperature and air movement on the  
flux of elemental mercury from substrate to the atmosphere, *Journal of Geophysical  
Research-Atmospheres*, 102(D3), 3891-3898.
- Gustin, M. S., S. E. Lindberg, and P. J. Weisberg (2008), An update on the natural sources and sinks  
of atmospheric mercury, *Applied Geochemistry*, 23, 482-493.
- Gustin, M. S., S. E. Lindberg, K. Austin, M. Coolbaugh, A. Vette, and H. Zhang (2000), Assessing the  
contribution of natural sources to regional atmospheric mercury budgets, *Science of the Total  
Environment*, 259, 61-71.
- Gustin, M. S., M. Engle, J. Ericksen, S. Lyman, J. Stamenkovic, and M. Xin (2006), Mercury  
exchange between the atmosphere and low mercury containing substrates, *Applied  
Geochemistry*, 21(11), 1913-1923.

- Gustin, M. S., et al. (1999), Nevada STORMS project: Measurement of mercury emissions from naturally enriched surfaces, *Journal of Geophysical Research-Atmospheres*, *104*(D17), 21831-21844.
- Hanson, P. J., S. E. Lindberg, T. A. Tabberer, J. G. Owens, and K. H. Kim (1995), Foliar exchange of mercury-vapor: Evidence for a compensation point, *Water Air and Soil Pollution*, *80*(1-4), 373-382.
- Hauke, V., and L. Schreiber (1998), Ontogenetic and seasonal development of wax composition and cuticular transpiration of ivy (*Hedera helix* L.) sun and shade leaves, *Planta*, *207*(1), 67-75.
- Kim, K. H., M. Y. Kim, J. Kim, and G. Lee (2002), The concentrations and fluxes of total gaseous mercury in a western coastal area of Korea during late March 2001, *Atmospheric Environment*, *36*(21), 3413-3427.
- Kim, K. H., M. Y. Kim, J. Kim, and G. Lee (2003), Effects of changes in environmental conditions on atmospheric mercury exchange: Comparative analysis from a rice paddy field during the two spring periods of 2001 and 2002, *Journal of Geophysical Research-Atmospheres*, *108*(D19).
- Kuiken, T., M. Gustin, H. Zhang, S. Lindberg, and B. Sedinger (2008a), Mercury emission from terrestrial background surfaces in the eastern USA. II: Air/surface exchange of mercury within forests from South Carolina to New England, *Applied Geochemistry*, *23*(3), 356-368.
- Kuiken, T., H. Zhang, M. Gustin, and S. Lindberg (2008b), Mercury emission from terrestrial background surfaces in the eastern USA. Part I: Air/surface exchange of mercury within a southeastern deciduous forest (Tennessee) over one year, *Applied Geochemistry*, *23*(3), 345-355.
- Lawrence, J. E., and G. M. Hornberger (2007), Soil moisture variability across climate zones, *Geophysical Research Letters*, *34*.
- Lindberg, S., R. Bullock, R. Ebinghaus, D. Engstrom, X. B. Feng, W. Fitzgerald, N. Pirrone, E. Prestbo, and C. Seigneur (2007), A synthesis of progress and uncertainties in attributing the sources of mercury in deposition, *Ambio*, *36*(1), 19-32.

- Lindberg, S. E., W. J. Dong, and T. Meyers (2002), Transpiration of gaseous elemental mercury through vegetation in a subtropical wetland in Florida, *Atmospheric Environment*, 36(33), 5207-5219.
- Lindberg, S. E., K. H. Kim, T. P. Meyers, and J. G. Owens (1995), Micrometeorological gradient approach for quantifying air-surface exchange of mercury-vapor: Tests over contaminated soils, *Environmental Science & Technology*, 29(1), 126-135.
- Lindberg, S. E., P. J. Hanson, T. P. Meyers, and K. H. Kim (1998), Air/surface exchange of mercury vapor over forests - The need for a reassessment of continental biogenic emissions, *Atmospheric Environment*, 32(5), 895-908.
- Lindberg, S. E., T. P. Meyers, G. E. Taylor, R. R. Turner, and W. H. Schroeder (1992), Atmosphere-surface exchange of mercury in a forest: Results of modeling and gradient approaches, *Journal of Geophysical Research-Atmospheres*, 97(D2), 2519-2528.
- Lindberg, S. E., W. J. Dong, J. Chanton, R. G. Qualls, and T. Meyers (2005), A mechanism for bimodal emission of gaseous mercury from aquatic macrophytes, *Atmospheric Environment*, 39(7), 1289-1301.
- Lindberg, S. E., et al. (1999), Increases in mercury emissions from desert soils in response to rainfall and irrigation, *Journal of Geophysical Research-Atmospheres*, 104(D17), 21879-21888.
- Magarelli, G., and A. H. Fostier (2005), Influence of deforestation on the mercury air/soil exchange in the Negro River Basin, *Amazon, Atmospheric Environment*, 39, 7518-7528.
- Mao, H., R. W. Talbot, J. M. Sigler, B. C. Sive, and J. D. Hegarty (2008), Seasonal and diurnal variations of Hg degrees over New England, *Atmospheric Chemistry and Physics*, 8(5), 1403-1421.
- Marsik, F. J., G. J. Keeler, S. E. Lindberg, and H. Zhang (2005), Air-surface exchange of gaseous mercury over a mixed sawgrass-cattail stand within the Florida Everglades, *Environmental Science & Technology*, 39(13), 4739-4746.
- McMillen, R. T. (1988), An eddy-correlation technique with extended applicability to non-simple terrain, *Boundary-Layer Meteorology*, 43(3), 231-245.

- Moeckel, C., G. O. Thomas, J. L. Barber, and K. C. Jones (2008), Uptake and storage of PCBs by plant cuticles, *Environmental Science & Technology*, 42(1), 100-105.
- Monteith, J. L. (1973), *Principles of environmental physics*, xiv, 241 p. pp., New York.
- Moore, C., and A. Carpi (2005), Mechanisms of the emission of mercury from soil: Role of UV radiation, *Journal of Geophysical Research-Atmospheres*, 110(D24).
- Moore, C. W. (2007), A survey of mercury in the brook trout and stream waters of the Shenandoah National Park, Virginia, Thesis, Master's Thesis, University of Virginia, 1-92.
- Nacht, D. M., and M. S. Gustin (2004), Mercury emissions from background and altered geologic units throughout Nevada, *Water Air and Soil Pollution*, 151(1-4), 179-193.
- National Atmospheric Deposition Program (NRSP-3), 2009. NADP Program Office, Illinois State Water Survey, 2204 Griffith Dr., Champaign, IL 61820.
- Obrist, D. (2007), Atmospheric mercury pollution due to losses of terrestrial carbon pools?, *Biogeochemistry*, 85(2), 119-123.
- Obrist, D., F. Conen, R. Vogt, R. Siegwolf, and C. Alewell (2006), Estimation of Hg-0 exchange between ecosystems and the atmosphere using Rn-222 and Hg-0 concentration changes in the stable nocturnal boundary layer, *Atmospheric Environment*, 40(5), 856-866.
- Poissant, L., and A. Casimir (1998), Water-air and soil-air exchange rate of total gaseous mercury measured at background sites, *Atmospheric Environment*, 32, 883-893.
- Poissant, L., M. Pilote, E. Yumvihoze, and D. Lean (2008), Mercury concentrations and foliage/atmosphere fluxes in a maple forest ecosystem in Quebec, Canada, *Journal of Geophysical Research-Atmospheres*, 113(D10).
- Poissant, L., M. Pilote, P. Constant, C. Beauvais, H. H. Zhang, and X. H. Xu (2004a), Mercury gas exchanges over selected bare soil and flooded sites in the bay St. Francois wetlands (Quebec, Canada), *Atmospheric Environment*, 38(25), 4205-4214.
- Poissant, L., M. Pilote, X. H. Xu, H. Zhang, and C. Beauvais (2004b), Atmospheric mercury speciation and deposition in the Bay St. Francois wetlands, *Journal of Geophysical Research-Atmospheres*, 109(D11).

- Poissant, L., M. Pilote, C. Beauvais, P. Constant, and H. H. Zhang (2005), A year of continuous measurements of three atmospheric mercury species (GEM, RGM and Hg-p) in southern Quebec, Canada, *Atmospheric Environment*, 39(7), 1275-1287.
- Rea, A. W., S. E. Lindberg, T. Scherbatskoy, and G. J. Keeler (2002), Mercury accumulation in foliage over time in two northern mixed-hardwood forests, *Water Air and Soil Pollution*, 133(1-4), 49-67.
- Riederer, M., and C. Müller (2006), *Biology of the plant cuticle*, xviii, 438 p., [436] p. of plates pp., Blackwell Pub., Oxford ; Ames, Iowa.
- Schreiber, L. (2005), Polar paths of diffusion across plant cuticles: New evidence for an old hypothesis, *Annals of Botany*, 95(7), 1069-1073.
- Schroeder, W. H., and J. Munthe (1998), Atmospheric mercury - An overview, *Atmospheric Environment*, 32(5), 809-822.
- Schroeder, W. H., S. Beauchamp, G. Edwards, L. Poissant, P. Rasmussen, R. Tordon, G. Dias, J. Kemp, B. Van Heyst, and C. M. Banic (2005), Gaseous mercury emissions from natural sources in Canadian landscapes, *Journal of Geophysical Research-Atmospheres*, 110(D18).
- Song, X. X., and B. Van Heyst (2005), Volatilization of mercury from soils in response to simulated precipitation, *Atmospheric Environment*, 39, 7494-7505.
- Stamenkovic, J., and M. S. Gustin (2009), Nonstomatal versus stomatal uptake of atmospheric mercury, *Environmental Science and Technology*, 43(5), 1367-1972.
- Stamenkovic, J., M. S. Gustin, J. A. Arnone, D. W. Johnson, J. D. Larsen, and P. S. J. Verburg (2008), Atmospheric mercury exchange with a tallgrass prairie ecosystem housed in mesocosms, *Science of the Total Environment*, 406(1-2), 227-238.
- Valente, R. J., C. Shea, K. L. Humes, and R. L. Tanner (2007), Atmospheric mercury in the Great Smoky Mountains compared to regional and global levels, *Atmospheric Environment*, 41(9), 1861-1873.

- Wallschläger, D., R. R. Turner, J. London, R. Ebinghaus, H. H. Kock, J. Sommar, and Z. F. Xiao (1999), Factors affecting the measurement of mercury emissions from soils with flux chambers, *Journal of Geophysical Research-Atmospheres*, *104*(D17), 21859-21871.
- Webb, E. K., G. I. Pearman, and R. Leuning (1980), Correction of flux measurements for density effects due to heat and water-vapor transfer, *Quarterly Journal of the Royal Meteorological Society*, *106*(447), 85-100.
- Xiao, Z. F., J. Munthe, W. H. Schroeder, and O. Lindqvist (1991), Vertical fluxes of volatile mercury over forest soil and lake surfaces in Sweden, *Tellus Series B-Chemical and Physical Meteorology*, *43*(3), 267-279.
- Xin, M., M. Gustin, and D. Johnson (2007), Laboratory investigation of the potential for re-emission of atmospherically derived Hg from soils, *Environmental Science & Technology*, *41*(14), 4946-4951.
- Zhang, H., S. E. Lindberg, and T. Kuiken (2008), Mysterious diel cycles of mercury emission from soils held in the dark at constant temperature, *Atmospheric Environment*, *42*(21), 5424-5433.
- Zhang, H., S. E. Lindberg, F. J. Marsik, and G. J. Keeler (2001), Mercury air/surface exchange kinetics of background soils of the Tahquamenon River watershed in the Michigan Upper Peninsula, *Water Air and Soil Pollution*, *126*(1-2), 151-169.
- Zhang, H. H., L. Poissant, X. H. Xu, and M. Pilote (2005), Explorative and innovative dynamic flux bag method development and testing for mercury air-vegetation gas exchange fluxes, *Atmospheric Environment*, *39*(39), 7481-7493.

## CHAPTER 3

# Seasonal contribution of dewfall to mercury deposition determined using a micrometeorological technique and dew chemistry

---

### Abstract

Wetted surfaces can augment mercury (Hg) deposition to soils and vegetation, and the magnitude of the total Hg deposition can vary seasonally. Dew is not typically accounted for in Hg budgets but little research has been done to determine if it is a significant deposition pathway. This study determined the relative importance of Hg deposition to dew with respect to rainfall and dry deposition on a seasonal basis at a remote site in Shenandoah National Park, VA. Dew samples were collected and analyzed for Hg concentrations ( $\text{ng L}^{-1}$ ) and dew depths (mm) were calculated using a micrometeorological approach based on the surface energy budget. Concentrations of Hg in dew (mean:  $5.57 \text{ ng L}^{-1}$ ) were lower than those observed in rainfall (mean weekly composite samples:  $8.80 \text{ ng L}^{-1}$ ). When deposition patterns were scaled to the seasonal and annual level, Hg deposition from rainfall was estimated to be 2-3 orders of magnitude greater than deposition to dew (2008 annual rainfall deposition:  $\sim 12400 \text{ ng m}^{-2}$ ; estimated annual Hg deposition to dew/frost:  $\sim 120 \text{ ng m}^{-2}$ ). The large disparity in magnitude between the two deposition pathways is attributed to the large amount of rainfall the site receives (2008 precipitation:  $\sim 1400 \text{ mm}$ ) in comparison to the total dewfall (estimated cumulative dew depth:  $\sim 20 \text{ mm}$ ). Scaled annual GEM fluxes were of the same order magnitude as deposition from rainfall, but indicated net emission from the site ( $\sim 4500 \text{ ng m}^{-2}$  emitted). Therefore, at sites with similar precipitation patterns, dew is not likely to significantly contribute to the total Hg deposition.

## 1. Introduction

Atmospheric mercury (Hg) deposition is a growing global concern, even in pristine regions far from point sources. Gaseous elemental mercury (GEM,  $\text{Hg}^0$ ) has an atmospheric lifetime on the order of one year allowing for long-distance transport and deposition (Schroeder and Munthe, 1998). It can subsequently be transformed into the potent neurotoxin methylmercury, which is a hazard to humans and wildlife (Mahaffey et al., 1997; Wolfe et al., 1998). Hg can be deposited from the atmosphere to the terrestrial environment via wet processes (e.g. entrained in rain droplets) or dry processes (e.g. direct deposition to surfaces from the atmosphere). Deposition to a wetted surface can be considered a special case of dry deposition, since the Hg dissolves only after it has been deposited. Gaseous oxidized mercury (GOM, any gaseous compound involving  $\text{Hg}^{2+}$ ) is considerably more soluble in water than GEM (Henry's Law coefficients at 20°C for  $\text{Hg}^0$  and  $\text{HgCl}_2$ :  $K_{\text{Hg}^0} = 729$  and  $K_{\text{Hg}(\text{Cl})_2} = 3.69 \times 10^{-5}$ , respectively; Schroeder and Munthe, 1998). Therefore dry deposition to a wetted surface is likely to involve primarily GOM or particulate-bound Hg ( $\text{Hg}_p$ ) species rather than GEM. There have been reports of reduced GOM concentrations at night over natural surfaces (Sheu and Mason, 2001; Weiss-Penzias et al., 2009), coincident with the timing of dew formation (Malcolm and Keeler, 2002). Here, we quantify the deposition of Hg in dew to a meadow in Shenandoah National Park using a micrometeorological (MM) technique combined with manual sampling of the dew chemistry. Our objective is to estimate how much Hg is deposited in this form on a seasonal and annual basis and to characterize its significance relative to other depositional pathways.

Dew formation occurs when a surface undergoes radiative cooling, and the surface temperature drops below the dew point allowing for water condensation from the warmer overlying atmosphere (Jacobs et al., 1994). In most locations, dew accounts for a small fraction the water balance, as the deposited water evaporates on daily timescales. It can, however, augment trace metal deposition if any dissolved metals are left behind after the water evaporates. Previous studies of major ions including some metals (e.g.  $\text{Ca}^{2+}$ ,  $\text{Mg}^{2+}$ ) in dew noted concentrations similar or greater than those of rainfall (Mulawa et al., 1986; Wagner and Steele, 1992).

There has only been one published study on Hg deposition related to dewfall. Malcolm and Keeler (2002) collected dew samples from three sites in the Great Lakes region and one site in the Florida Everglades. Hg concentrations in dew were lowest at a remote location near Lake Superior (Eagle Harbor, MI, where the mean Hg concentration was  $2.8 \pm 2.4 \text{ ng L}^{-1}$ ) and highest in the Everglades (mean Hg concentration:  $6.0 \pm 4.9 \text{ ng L}^{-1}$ ). Concentrations within all of the collected samples varied by an order of magnitude (range:  $1.0$  to  $22.6 \text{ ng L}^{-1}$ ). In general, the Hg levels in dew were lower than those in precipitation (three-month rainfall mean for three Great Lakes sites:  $15.2 \pm 10.0$ ,  $8.9 \pm 6.7$  and  $13.0 \pm 14.8 \text{ ng L}^{-1}$ ). The volume of dew formed can also affect the total Hg deposition to a site, rendering it more or less significant in comparison to rainfall. In the Everglades during the dry season, total Hg deposition ( $\text{ng m}^{-2}$ ) from dew was estimated to be approximately equal to the Hg deposition from rainfall (Malcolm and Keeler, 2002), suggesting that it is an important deposition pathway during a portion of the year.

The limited research incorporating dew into the Hg cycle could be related to the challenges associated with dew collection. There is no standard measurement technique for estimating the dew depth (volume of dew/surface area, [length]). The volume of dew collected is highly dependent on the sampling surface and is likely to differ significantly from natural plant and ground surfaces. Sampling methods currently in use include visual, volumetric, and gravimetric techniques (Skarzynska et al., 2006). Many volumetric and gravimetric methods rely on a flat polytetrafluoroethylene (PTFE) sheet exposed to the atmosphere to collect dew. However, the underlying materials (Styrofoam, wood, or metal) and the height of the sampler can block or assist heat transfer from the surface to the atmosphere, augmenting or diminishing dew formation. Takenaka et al. (2003) used several different dew sampling methods, and found varying dew depths depending on the measurement technique. In addition, the measured dew depth will be affected by the time of sample collection. Maximum dew depth is generally thought to occur at dawn, but Kidron (2000) noted that dew condensation continues after sunrise at some sites.

A micrometeorological method to determine maximum dew depth would better reflect the true extent of dew formation on the natural land surface and would also allow for the development of

longer-term data sets. Dew estimates from eddy-covariance (EC) techniques are often not reliable and underestimate dew formation (Moro et al., 2007). These measurements rely upon adequately turbulent conditions, and there is increased measurement uncertainty during periods with low wind speeds as commonly encountered during the nighttime when stable conditions are favorable for dew formation. A surface energy budget (SEB) model does not require turbulent conditions, and therefore produces more reliable results during these periods (Holtslag and de Bruin, 1988). Jacobs et al. (2006) developed a dew formation model based on the SEB and tested it over a short canopy (10 cm) grassland in the Netherlands. Results were compared to microlysimeters weighed at 30 minute increments to detect small changes in mass, indicative of dew deposition or evasion. The dew model matched within 2% of the experimental collection, and the model was considered acceptable for all four seasons, but generally less reliable during frost or snowy conditions.

Analyzing dew for Hg concentration in tandem with the SEB model for dew depth over natural surfaces would provide a better estimate for Hg fluxes associated with dew formation. Therefore, the purpose of this study is to: (1) quantify Hg concentrations in dew at a remote location in Shenandoah National Park on a seasonal basis, (2) use micrometeorological techniques to determine dew depth, and (3) determine the relative importance of mercury deposition in dew with respect to rainfall and other forms of dry deposition at this site.

## **2. Materials and Methods**

### *2.1 Site Description*

Big Meadows within Shenandoah National Park, VA is a relatively open flat area, containing two wetlands. It is the largest open region within the park and is at a high elevation (1050 m). The meadow consists of low-lying, non-woody vegetation. Common plant species include sedges (*Carex spp.*), lowbush blueberry (*Vaccinium pallidum*), and bent grass (*Agrostis capillaries*) (Wendy Cass, personal communication). Weeklong field campaigns were completed during each season: August 6-12, 2008 (summer), November 5-14, 2008 (fall), February 9-17, 2009 (winter), and May 11-19, 2009 (spring). The canopy height was approximately 60 cm in the summer and fall, 30 cm in the winter, and 40 cm in the spring.

Big Meadows is also a national Mercury Deposition Network site, with bulk rainfall Hg concentrations recorded on a weekly basis since 2002. The meadow is not situated near to an atmospheric point source for Hg and has low soil mercury concentrations of approximately  $0.10 \mu\text{g g}^{-1}$  in the upper 0.05 m of the soil profile.

## 2.2 Dew model theory

The basic premise for the SEB model is to calculate the flux density of evaporation/dew formation,  $E$  [ $\text{kg m}^{-2} \text{s}^{-1}$ ], for each measurement period without using techniques that necessitate turbulent conditions. The equations used in the model are included here, but a more detailed description including potential applications are available in Jacobs et al. (2006). The original equation for the model is the surface energy budget:

$$\lambda_v E = R_n - G - H \quad (1)$$

where  $\lambda_v$  is latent heat of vaporization [ $\text{J kg}^{-1}$ ],  $R_n$  is net radiation [ $\text{W m}^{-2}$ ],  $G$  is soil heat flux [ $\text{W m}^{-2}$ ], and  $H$  is sensible heat flux [ $\text{W m}^{-2}$ ]. This is combined with the equation for free water vapor evaporation/dew formation (Garratt and Segal, 1988) and Penman's substitution (Garratt, 1992) to solve for the evaporation or dew formation:

$$E = \left[ \frac{s}{s+\gamma} (R_n - G) + \frac{\gamma}{s+\gamma} \frac{\rho \lambda_v \delta q}{r_{av}} \right] / \lambda_v \quad (2)$$

where  $s = dq^*/dT$  is the slope of a saturation specific humidity curve [ $\text{Pa K}^{-1}$ ],  $\gamma$  is the psychrometric constant [ $\text{Pa K}^{-1}$ ],  $\rho$  is air density [ $\text{kg m}^{-3}$ ],  $\delta q = q^*(T_r) - q$  is the specific humidity deficit at the reference level [ $\text{kg kg}^{-1}$ ],  $T_r$  is the air temperature at the reference level, and  $r_{av}$  is the aerodynamic resistance to water vapor [ $\text{s m}^{-1}$ ]. The aerodynamic resistance to water vapor,  $r_{av}$ , is determined using (Garratt, 1992):

$$r_{av} = \left( \ln \left( \frac{z_r}{z_{ov}} \right) - \Psi_v(\eta_r) + \Psi_v(\eta_{ov}) \right) \left( \ln \left( \frac{z_r}{z_o} \right) - \Psi_m(\eta_r) + \Psi_m(\eta_o) \right) / \kappa^2 u_r \quad (3)$$

where  $z_o$  and  $z_{ov}$  are the momentum and water vapor momentum roughness lengths, respectively [m],  $\Psi_m$  and  $\Psi_v$  are the momentum and water vapor stability functions, respectively,  $\eta_r = z_r/L$ ,  $\eta_{ov} = z_{ov}/L$ ,  $\eta_o = z_o/L$ ,  $L$  is the Obukhov length [m],  $\kappa$  is von Karman's constant, and  $u_r$  is the wind speed at the

reference height [ $\text{m s}^{-1}$ ]. The Obukhov length and stability functions are determined using the bulk Richardson number,  $Ri_B$  (de Bruin et al., 2000), and do not rely on eddy covariance methods (Jacobs et al., 2006).

The total depth of dew,  $D$  [mm], is determined by summing the negative evaporation (indicative of dew deposition) at each time step ( $i$ ).

$$D_{i+1} = \begin{cases} D_i + 10^3 E_i \Delta t / \rho & \text{if } D_i + 10^3 E_i \Delta t / \rho \geq 0 \\ 0 & \text{if } D_i + 10^3 E_i \Delta t / \rho < 0 \end{cases} \quad (4)$$

Once  $D_{i+1}$  equals zero, all of the free water on the canopy surface has evaporated. Any evaporation during dry surface conditions would involve transpiration from plants and must take into account the canopy resistance ( $r_c$ ), which was not incorporated into the model. All of the variables in the above equations are recorded using standard flux tower equipment, making it potentially useful for widespread applications.

### 2.3 Micrometeorological instrumentation

A portable flux tower was placed at the same location (38°30'54" N, 78°26'04"W) in each of the four seasons, positioned at the center of the meadow to ensure adequate fetch.

Micrometeorological instruments used for eddy covariance measurements were mounted at a height of 2.41 meters. Wind speed, temperature and specific humidity were measured using a triaxial sonic anemometer (CSAT3, Campbell Scientific, Inc.) in tandem with an open path  $\text{H}_2\text{O}$  and  $\text{C}_2\text{O}$  analyzer (Li7500, Li-Cor, Inc.). Net short and long wave radiation were measured with a net radiometer (CNR1, Kipp & Zonen). Surface temperature was recorded with two infrared temperature sensors (model IRTS-S, Apogee Instruments, Inc.) pointed at the grass surface and corrected for IRT body temperature. The IRT sensors tended to malfunction during foggy or rainy conditions, requiring the plant surface temperature to be approximated during these periods using the soil temperature at 0.025 cm depth, as suggested by Jacobs et al. (2006). Soil temperatures were measured in duplicate at depths of 0.025 and 0.075 cm with glass insulated thermocouples (5TC-GG series, Omega, Inc.). Soil moisture was measured by a pair of time domain reflectrometers (CS616-L, Campbell Scientific, Inc.) at depths of 0.05 m and 0.30 m. Duplicate soil heat flux plates were buried at 0.05 m depth (HFT3-L,

Campbell Scientific, Inc.), and a dielectric leaf wetness sensor (LWS-L, Campbell Scientific, Inc.) was positioned 0.5 m above the ground surface.

GEM concentrations were measured concurrently at two heights (1.31 m and 3.05 m) using an ambient air analyzer (2537B, Tekran Inc.) and GEM fluxes were determined using a micrometeorological technique known as the aerodynamic method. This technique is based on Monin-Obukov similarity theory, in which measurements of the vertical gradient of a scalar can be related to fluxes from/to the surface (Baldocchi et al., 1988). This method has previously been applied to Hg flux measurements (e.g. Edwards et al., 2005), and specific details regarding these GEM flux measurements at this site are provided elsewhere (Converse et al., submitted). All data were averaged on a data logger at 20-minute intervals.

#### *2.4 Dew collection*

As there is no standard protocol for dew collection for ion analysis, methods were chosen based on use in prior studies, ease of collection, and minimizing the possibility for contamination. The dew collector consisted of a 1.5 m<sup>2</sup> thin Teflon sheet mounted on a large board of Styrofoam secured to a table at 0.8 m above the ground. Approximately 30 minutes before sunset, the Teflon was washed as described below to remove possible Hg contamination to the film. If there was no precipitation during the evening, dew was collected the following morning approximately 30 minutes before sunrise. Dew was pushed to the center of the sheet using a fabricated Teflon squeegee, which was washed in the same manner as the Teflon film before each use. The Styrofoam board was hinged down the middle to facilitate pouring and sample collection. Frost samples were collected in the same fashion. Although every effort was made to collect the entire dew sample, certain evenings produced more than 250 mL of dew (exceeding the sample bottle size) resulting in sample loss during the collection procedure. Field blanks were collected by pouring 250 mL of deionized water directly onto the Teflon sheet and following the above sampling protocol. Trip blanks were collected by pouring deionized water directly into sample bottles. The Teflon sample bottles were acid washed following the EPA protocol for aqueous Hg sample collection (EPA, Method 1631, 2002). Samples were preserved with 100% BrCl to prevent Hg evasion (1.25 mL BrCl per 250 mL sample) and analyzed

for Hg by cold vapor-atomic fluorescence (CVAFS, model 2600, Tekran, Inc.) within 30 days of collection at the University of Virginia.

The washing protocol for the Teflon membrane suggested by Malcolm and Keeler (2002) was used in the summer sampling, but was later modified due to high Hg concentrations in the field blanks. In the summer, the film was rinsed once with deionized water, twice with a 10% HCl solution, and once more with deionized water. After each washing, the surface was wiped dry with acid-resistant particle-free wipes. Samples were preserved onsite, and three field blanks were collected. We speculate that the onsite preservation with BrCl under non-clean room conditions led to the high Hg concentrations in some of the field blanks. The following three seasons, samples were capped and double bagged to await preservation with BrCl at the end of each campaign under semi-clean room conditions.

Laboratory testing revealed that simply washing with deionized water could produce reliable field blanks, similar to those after acid cleaning (data not shown). Therefore, in the fall, winter and spring, the Teflon sheet was washed three times with approximately 250 mL of deionized water. Excess water was poured onto the ground, and the surface was wiped dry with acid-resistant particle-free wipes before deployment. The number of field blanks was also increased to one per night.

### *2.5 Computation and statistical analysis*

All data analysis was completed using Matlab R2008b (The Mathworks, Inc.) and statistical analysis was completed using SPSS Statistics 17.0 (SPSS, Inc.). A one-way analysis of variance (ANOVA, Tukey post hoc) was used to compare mean values, and statistical relationships were assumed significant at  $p < 0.05$ . Any subsequent use of the  $\pm$  symbol indicates the standard deviation from the mean.

## **3. Results**

### *3.1 Environmental conditions and data post-processing*

Fair weather dominated during the week-long summer sampling, foggy conditions prevailed in the fall, strong winds and light snow showers occurred in the winter, and heavy rains storms passed

through the meadow in the spring. Air temperatures remained below 0°C for a number of days in winter and for several nights in the fall and spring. There were several instances in which rain and fog caused the open path H<sub>2</sub>O and C<sub>2</sub>O analyzer (Licor) to malfunction, requiring such data to be removed. Water vapor flux determined using eddy covariance was also measured for comparison with the SEB model. For these measurements, axis rotations were applied to correct for any instrument misalignment (McMillen, 1988) and Webb-Pearman-Leuning (WPL) corrections were applied to all fluxes to account for air density effects (Webb et al., 1980).

### 3.2 Mercury levels in dew

Seven trip blanks and twenty-two field blanks were collected within the entire study. Trip blanks consistently had near zero Hg levels (mean: 0.08 ng L<sup>-1</sup>). Field blanks had the highest mean Hg concentration in the summer (3.60 ± 3.70 ng L<sup>-1</sup>) primarily due to one sample (7.87 ng L<sup>-1</sup>). Concentrations were greatly reduced in the following three seasons using the modified collection protocol (0.29 ± 0.25 ng L<sup>-1</sup>, 0.16 ± 0.08 ng L<sup>-1</sup>, and 0.26 ± 0.18 ng L<sup>-1</sup> in the fall, winter and spring, respectively). The mean water mass of the field blanks (198 g) was slightly larger than that of the dew samples. To account for the difference in volumes, all dew samples were corrected by subtracting the Hg mass (rather than concentration) of the seasonal mean trip blank and the field blank collected immediately prior to the Teflon sheet deployment.

A total of 14 dew samples (9 liquid dew and 5 frost samples from 27 collection attempts) were collected over all four campaigns (Figure 1). Collection could not be completed when there was not significant dew accumulation on the table, if the dew table was compromised by strong winds, or if there was overnight precipitation. The amount of dew collected on an individual morning ranged from 5 to 450, with a mean of 187 g. For the night of the largest dew formation (~450 g sample), two collection bottles were used. One frost sample weighing ~5 g was not analyzed for Hg concentration due to the small sample volume.

The mean Hg concentration in all samples was 5.57 ± 4.45 ng L<sup>-1</sup>, with both the maximum (12.42 ng L<sup>-1</sup>) and minimum (0.12 ng L<sup>-1</sup>) values occurring in the summer. The mean Hg mass deposited in each dew event was 0.53 ± 0.51 ng m<sup>-2</sup>. Seasonal mean Hg concentrations are listed in

Table 1. Differences between seasons were not statistically significant for either Hg concentration ( $p = 0.35$ ) or total Hg deposition ( $p = 0.99$ ), perhaps owing to the limited sample size.

Frost samples had significantly higher Hg concentrations than liquid dew samples with mean values of  $10.39 \pm 1.01 \text{ ng L}^{-1}$  and  $3.42 \pm 3.54 \text{ ng L}^{-1}$ , respectively ( $p = 0.03$ ). However, there was not a not significant difference in mass of Hg deposited in dew compared to frost ( $p = 0.74$ ), as frost samples were significantly smaller than dew (mean mass of  $64 \pm 19 \text{ g}$  and  $241 \pm 96 \text{ g}$ , respectively).

### 3.3 Atmospheric GEM concentrations and GEM fluxes

Seasonal GEM concentrations were measured and fluxes calculated during the same time period as dew collection. This allowed for a site-specific comparison of the magnitude of nighttime GEM fluxes to Hg deposited to the wetted surface. GEM concentrations remained low with seasonal means of  $1.27 \pm 0.10$ ,  $1.28 \pm 0.07$ ,  $1.38 \pm 0.09$ , and  $1.19 \pm 0.12 \text{ ng m}^{-3}$ , in the summer, fall, winter and spring, respectively. These values are comparable to other concentrations at remote grassland sites (Fritsche et al., 2008), but slightly lower than the many values reported for remote/rural regions in the Northern Hemisphere ( $1.5\text{-}1.8 \text{ ng m}^{-3}$ , Valente et al., 2007). Atmospheric GEM concentration nearest to the time of collection or the mean value of the previous night were not significantly correlated with Hg concentration in dew ( $p = 0.72$  and  $p = 0.88$ , respectively) or with the mass of Hg deposited ( $p = 0.30$  and  $0.32$ , respectively). Figure 1b displays the Hg concentrations in dew samples together with atmospheric GEM concentrations measured continuously onsite.

The cumulative GEM fluxes ( $\text{ng m}^{-2}$ ) the night prior to dew collection were not significantly correlated with either Hg concentrations ( $p = 0.35$ ) or the mass of Hg deposited in dew ( $p = 0.98$ ). Figure 2 displays the nighttime GEM flux in tandem with the Hg deposition attributed to dew formation. Additional details regarding the GEM flux measurements and interpretation of these dynamics are reported in Converse et al. (submitted).

### 3.4 Dew depth from MM measurements

Dew depths with the SEB model ranged from 0.00 to 0.25 mm (Figure 1) with the most frequent dew formation in the summer (Figure 3). The largest mean depth was in the summer and

spring, both having a mean of 0.071 mm. Note the high mean dew depth in the spring is largely attributed to one date (May 13). The EC technique measured smaller dew depths (ranging from 0 to 0.11 mm) than the SEB model. The mean dew depths for each season using the SEB model and EC technique are listed in Table 1. Depths measured by the SEB model are more in line with those estimated by physical collection (Figure 3b).

The SEB model typically estimated greater dew depths than those determined using the EC technique (21 of the 29 sampling nights). This was expected considering that nighttime periods are often less turbulent, resulting in underestimated water vapor fluxes using the EC method. The summer season best exemplified this tendency (Figure 3) when wind speeds were lowest compared with the other seasons.

Physical dew samples were collected on all nights when the SEB model predicted dew depths of at least 0.01 mm at the time of collection (assuming no rainfall overnight). Exceptions include August 5<sup>th</sup> (when the dew table was not ready for use), February 14<sup>th</sup>, and May 13<sup>th</sup>. On the later two dates, the SEB model predicted a substantial dew deposition (maximum depths of 0.14 mm and 0.25 mm) but there was no dew present on the collection table.

A wetness sensor was deployed as an independent check for the presence or absence of dew. The signal reading from the wetness sensor did not consistently track dew formation predicted by either method (Figure 3a). The shape of the wetness sensor peak and the location of the peak maximum sometimes coincided with the MM methods (e.g. August 7) but this was not uniform across nighttime periods.

## **4. Discussion**

### *4.1 Hg in dew, frost, and rainfall*

The mean Hg concentration in dew ( $5.57 \pm 4.45 \text{ ng L}^{-1}$ ) was larger than that reported at a remote site in Michigan ( $2.8 \pm 2.4 \text{ ng L}^{-1}$ ) and similar to those collected in the Florida Everglades ( $6.0 \pm 4.9 \text{ ng L}^{-1}$ ) (Malcolm and Keeler, 2002). The amount of Hg deposited per dew event was not statistically different between seasons ( $p = 0.99$ ). Furthermore, the mass of Hg in the sample was not statistically different between dew and frost ( $p = 0.74$ ), with a consistent amount of Hg deposited

to the wetted surface ( $0.53 \pm 0.51 \text{ ng m}^{-2}$ ) irrespective of the solvent phase. Malcolm and Keeler (2002) also did not see a significant difference in the mass of Hg deposited in dew and frost events. This suggests that the structural differences between solid and liquid water are not limiting Hg deposition. Although it is somewhat counterintuitive that the physical structure of the water would not affect how much Hg dissolves, it is likely that atmospheric GOM and  $\text{Hg}_p$  levels are limiting deposition. All further references to dewfall include both dew and frost measurements.

For all seasons, concentrations in dew were lower than the mean Hg levels in rainfall at Big Meadows. Within the Oct 2002-Dec 2008 period the local MDN site reported a mean concentration of Hg in rainfall of  $8.80 \pm 7.08 \text{ ng L}^{-1}$  (National Atmospheric Deposition Program (NRSP-3), 2009). The observation of lower Hg levels in dew versus rainfall was also reported by Malcolm and Keeler (2002) at all of their measurement locations. In combination with our results, this suggests that this trend is not site or season specific. More research is needed to determine if the proximity to a point source affects concentrations in dewfall, to the point that it may be enriched relative to rainfall. None of the reported measurements to date have been from an urban/industrial area, and these findings might only apply to remote/rural settings.

The difference in concentration between rainfall and dewfall could be attributed to different atmospheric source pools. The Hg in dew originated from the air mass directly above the land surface, while rainfall could have potentially scavenged Hg from higher, theoretically more Hg-rich regions of the troposphere. Swartzendruber et al. (2006) measured speciated Hg concentrations at the Mount Bachelor Observatory in Oregon and reported periodic nighttime enhancements in GOM (up to  $600 \text{ pg m}^{-3}$ ) that were linked to downslope winds that brought down free tropospheric air at night. They suggested that the increased GOM levels were caused by oxidation of the GEM species in the free troposphere by ozone or through different production mechanisms. It is possible that cloud droplets are episodically exposed to higher concentrations of GOM resulting in higher Hg levels in rainfall. In contrast, GOM levels near the surface (available for deposition to dewfall) are generally low with concentrations of  $\sim 3 \text{ pg m}^{-3}$  (Poissant et al, 2005).

Kolker et al. (2008) measured speciated Hg at Big Meadows for 10 days in 2006 and background GOM levels remained low ( $< 5 \text{ pg m}^{-3}$ ) for most of the sampling interval. However, there were two daytime periods with elevated GOM ( $>30 \text{ pg m}^{-3}$ ) that corresponded with peaks of  $\text{SO}_2$ . These episodes were thought to be plume events rather than *in situ* formation of GOM since concentrations increased and declined rapidly. If this pattern is a regular occurrence at the Big Meadows site (and happens at night), it could account for some of the variability in Hg deposition to dew.

#### 4.2 Temporal variability in dew Hg concentrations

Hg concentrations in dew exhibited some variability with no clear seasonal patterns. The mass of Hg deposited to dew was not significantly correlated to GEM concentrations on the night prior to dew collection, which were relatively constant at our site. This was not surprising, since as previously noted, we anticipate that GOM and  $\text{Hg}_p$  species are more likely to be deposited to a wetted surface. The temporal variability of GOM and  $\text{Hg}_p$  concentrations could be substantially different from that of GEM. Measurements of GOM or  $\text{Hg}_p$  concentrations concurrent with dew samples could be undertaken to determine if this is indeed the case.

There is no significant correlation between cumulative nighttime GEM fluxes and Hg deposition to dew (Figure 2). Cumulative nighttime GEM deposition fluxes were much larger in magnitude (range: 312 to -96  $\text{ng m}^{-2}$ ) compared with to Hg deposition to dewfall (range: 1.6 to 0  $\text{ng m}^{-2}$ ). Measurements of Hg levels in dew could be used as a proxy for GOM and  $\text{Hg}_p$  deposition to the surface, since GEM has low water solubility and is not likely to comprise a large fraction of the Hg levels in dew. Using this approximation, our site would be considered to be dominated by GEM fluxes.

It is not known if Hg deposited to dew is emitted back to the atmosphere as GEM when dew evaporates. We did not observe an emission pulse of GEM while the surface dried. Figure 4 displays the mean hourly nighttime GEM fluxes in tandem with mean hourly nighttime dew formation predicted using the SEB model. GEM emissions peaked later in the day roughly coinciding with solar noon, long after the surface dried. This suggests that the dew-deposited Hg: (1)

remained on the surface, (2) was volatilized as GOM and therefore not measured as part of the GEM fluxes, or (3) was volatilized as GEM, but the pulse was simply not large enough to be captured within the MM measurement technique. If the Hg deposited in dew remains on the surface, it would be considered a Hg input to the terrestrial system. If the Hg deposited to the surface is volatilized back to the atmosphere (as GOM or GEM), then dew formation is only a temporary store for Hg, and should not be considered an input in the terrestrial sphere.

#### *4.3 Relative significance of dew to Hg deposition*

Measurements of Hg levels in dew and net GEM fluxes were scaled to the seasonal level by assuming that our weeklong results are representative of the entire season. While it is recognized that dew depths and Hg concentrations are variable, this simple exercise offers an approximate magnitude of Hg deposition to dew and can provide insight as to whether dew formation is an important deposition pathway. Hg deposition estimates on a seasonal basis for dewfall, rainfall, and GEM fluxes are listed in Table (2).

At the Big Meadows site, the rainfall depth vastly outweighs that of dewfall; the latter only accounted for ~1.5% of the total water input. Although the Hg concentrations were similar between rain and dew, that amount of precipitation the site receives means that rainfall is the dominant pathway for dissolved Hg deposition. At other sites where dew accounts for a larger fraction of the water budget, Hg deposition to dewfall could play a larger role in Hg cycling. For example, some deserts contain enough moisture in the lower atmosphere for regular dew formation. The Negev Desert, at Sede Boker, Israel, annually receives ~17 mm of dew deposition and only ~90 mm of rainfall (Zangvil, 1996).

The seasonal GEM fluxes measured concurrently within this study were of the same magnitude as the deposition in rainfall, although some seasons recorded net atmospheric evasion from the site (indicated by negative deposition values in Table 2). The total Hg deposition from dewfall, likely to be the GOM species, is minimal in comparison to GEM dry deposition. As GEM constitutes the majority of all atmospheric Hg species at Big Meadows (>~95%, Kolker et al., 2008) the large disparity in magnitude between these pathways is not surprising. However, the fates of

deposited atmospheric GEM and the likely Hg species in dew could be substantially different. GEM is more likely to be released back to the atmosphere, while the charged GOM species, which are likely dominant in dew, could adsorb to vegetation and soil surfaces, remaining in the terrestrial environment for a longer period of time.

## 5. Summary

In 2008-09, we measured Hg concentrations in dew using traditional physical sampling techniques and modeled dew depth over natural surfaces using a MM approach. The SEB model adequately predicted dew deposition, and can be a useful tool for estimating dew formation over natural land surfaces using basic micrometeorological instrumentation. Concentrations of Hg in dew (mean:  $5.57 \text{ ng L}^{-1}$ ) were similar to those seen in rainfall, but the estimated yearly dew depth (~20 mm) was considerably less than the rainfall depth measured in 2008 (~1400 mm). Frost samples had significantly higher Hg concentrations than liquid dew samples, but there was not a significant difference in the mass of Hg deposited. Cumulative nighttime GEM fluxes on nights prior to dew formation were not correlated with Hg concentrations in dew. In addition, the diel patterns in GEM fluxes did not track dew formation (i.e. no GEM deposition signal at the onset of dew formation and no GEM emission pulse when dew evaporated). On a seasonal or yearly scale, the Hg deposition in rainfall and deposition/emission to the atmosphere are 2-3 orders of magnitude greater than Hg deposited into dewfall. In regions where dewfall depth is more comparable to rainfall depth, however, it could constitute a larger fraction of Hg deposition. Additional work is needed to determine if the Hg deposited in dew remains on the surface, or if it is released back to the atmosphere upon evaporation of the dew.

## Acknowledgments

Funding for this project was provided by the U.S. Department of Education's program for Graduate Assistance in Areas of National Need and the National Science Foundation Hydrologic Science Program (EAR-0645697). Aqueous mercury analysis instrumentation was funded by the Dominion Foundation and the University of Virginia. We would like to thank the Shenandoah

National Park Service staff for their support and advice, specifically Julena Campbell, Liz Garcia, and Jim Schaberl.

**Figure 1.** (a) Dew depth (mm) determined by both the SEB model and EC measurements. Dew depth determined by the EC method is typically lower than the SEB model. (b) Hg concentrations in dew samples ( $\text{ng L}^{-1}$ ) and atmospheric GEM concentrations ( $\text{ng m}^{-3}$ ). Frost samples are indicated by asterisks. Dark and light shading are present to differentiate seasons.

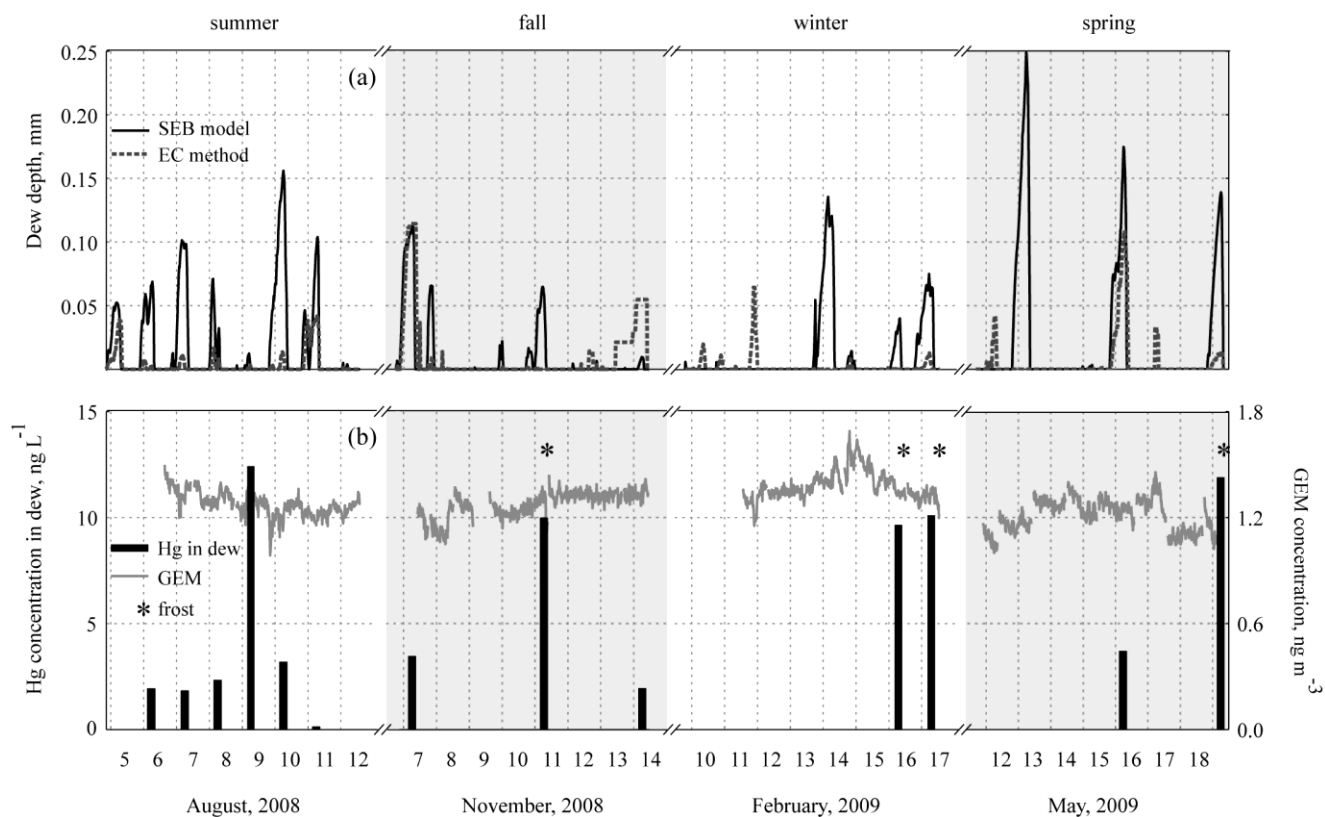


**Figure 2.** Cumulative nighttime atmospheric GEM fluxes [ $\text{ng m}^{-2}$ ] and estimated Hg deposition to dew [ $\text{ng m}^{-2}$ ]. GEM fluxes were determined using the aerodynamic method, with negative values indicating net emission from the surface. Hg deposition to dew was determined using the measured Hg concentration in collected dew samples and the maximum dew depth according to the SEB model. If a dew sample was not collected on a night (no Hg concentration available) the mean seasonal Hg concentration in dew was used. Note two order of magnitude differences in axes for the GEM fluxes and Hg deposition to dew. The springtime experienced a large GEM deposition event and therefore has a unique axis.

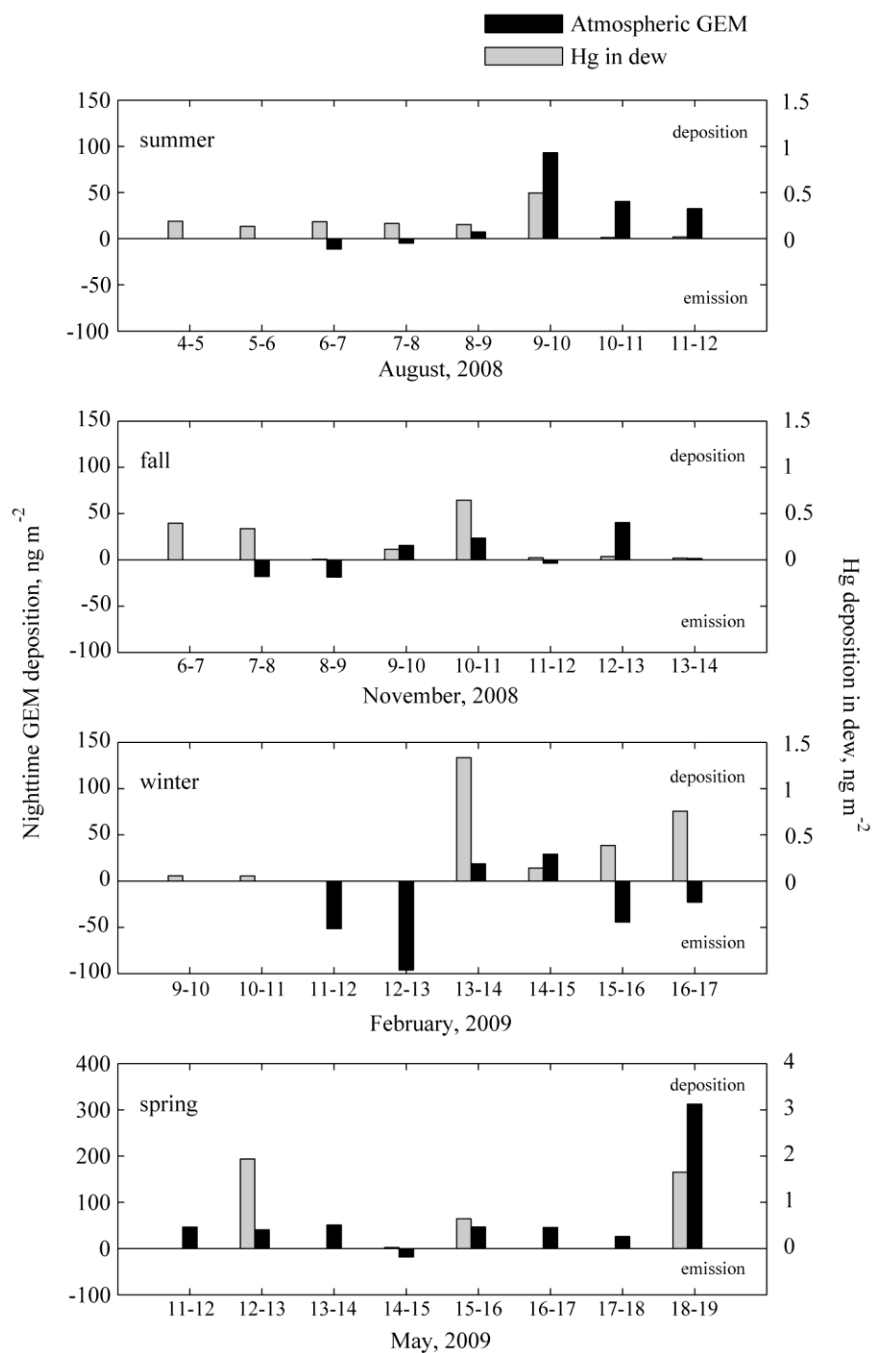


**Figure 3. (a)** Signal from the wetness sensor (mV). Mid-day showers on August 6<sup>th</sup> and 10<sup>th</sup> are marked with arrows. **(b)** Continuous dew depth (mm) as determined by the SEB model and EC measurements and the instantaneous dew depth as determined by physical collection (volume collected/table surface area). Note that the physical collection technique is not representative of dew formation on a natural surface, and therefore might not be directly comparable to MM methods.

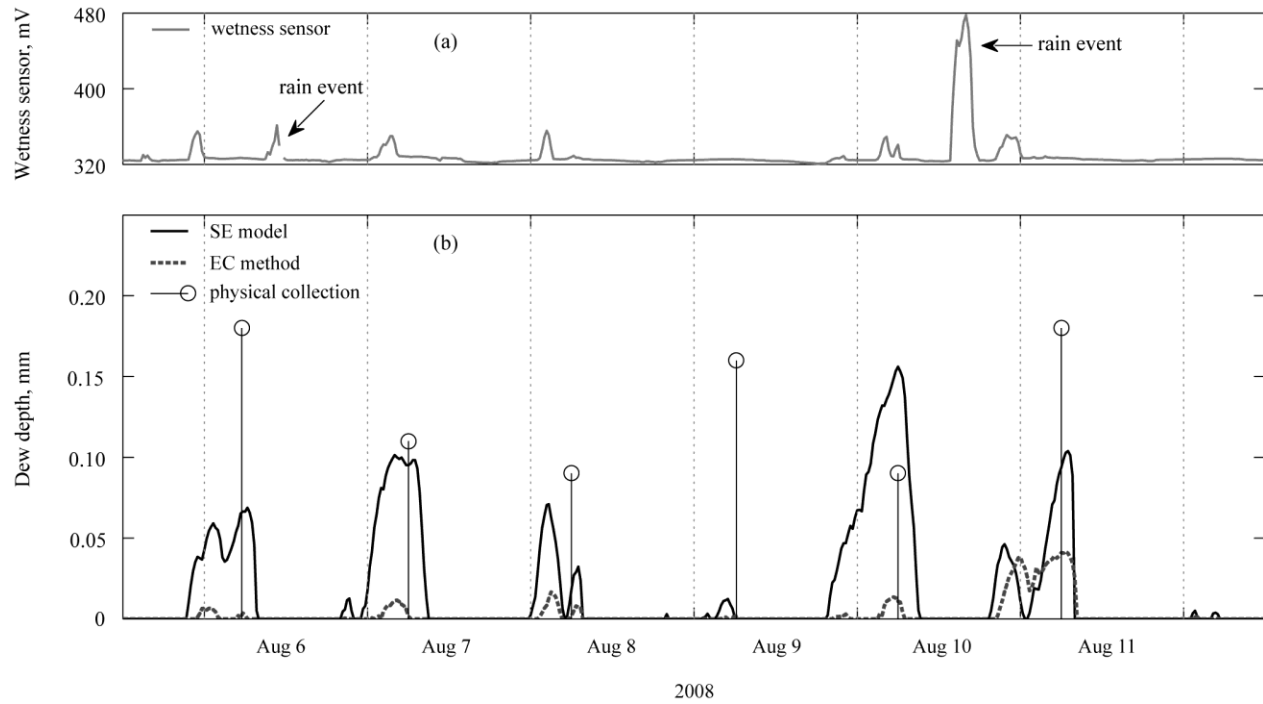


**Figure 4.** Nighttime averaged hourly GEM fluxes [ $\text{ng m}^{-2} \text{h}^{-1}$ ] and cumulative dew formation [mm] determined using the SEB model. Error bars on GEM fluxes denote  $\pm$  one standard deviation. There was not a pulse of GEM emissions while dew evaporated in the early morning.

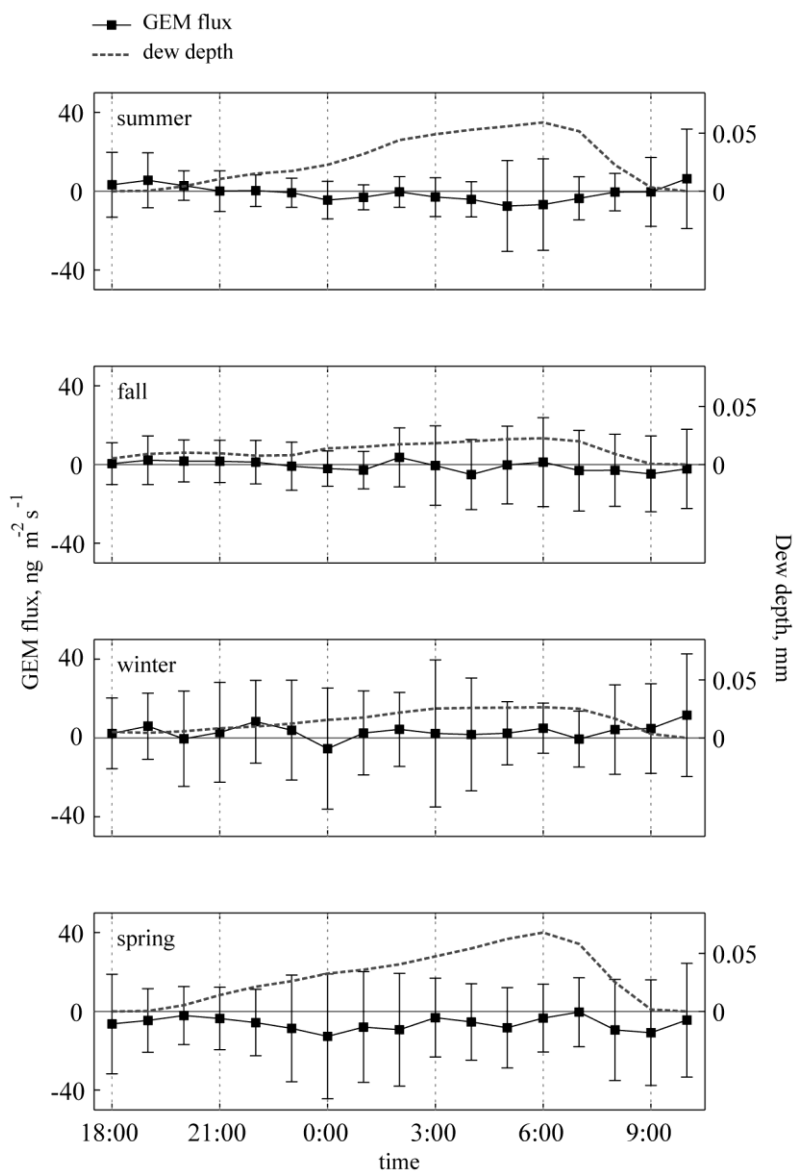


**Table 1.** Seasonal mean Hg concentrations in dew and mean modeled maximum dew depths.

|                | Number of dew samples | Mean Hg concentration<br>[ng L <sup>-1</sup> ] | Mean Hg deposition<br>[ng m <sup>-2</sup> ] | Mean maximum nightly dew depth [mm] |               |
|----------------|-----------------------|--|---|-------------------------------------|---------------|
|                |                       |  |   | SEB model                           | EC method     |
| <b>Summer</b>  | 6                     | 3.63 ± 4.42                                    | 0.51 ± 0.73                                 | 0.071 ± 0.050                       | 0.017 ± 0.016 |
| <b>Fall</b>    | 3                     | 5.11 ± 4.27                                    | 0.56 ± 0.41                                 | 0.036 ± 0.041                       | 0.029 ± 0.040 |
| <b>Winter</b>  | 2                     | 9.86 ± 0.32                                    | 0.45 ± 0.16                                 | 0.035 ± 0.048                       | 0.015 ± 0.021 |
| <b>Spring</b>  | 2                     | 7.78 ± 5.79                                    | 0.61 ± 0.01                                 | 0.071 ± 0.10                        | 0.025 ± 0.038 |
| <b>Overall</b> | 13                    | 5.57 ± 4.45                                    | 0.53 ± 0.51                                 | 0.053 ± 0.064                       | 0.021 ± 0.030 |

**Table 2.** Estimated seasonal deposition from rainfall and dew as well as estimated seasonal GEM fluxes. Seasonal designation was chosen based on the 2008 solstices and equinoxes. Rainfall depth and Hg concentration data are from the MDN station at Big Meadows (weekly composite samples, National Atmospheric Deposition Program (NRSP-3), 2009). Dry deposition estimates were derived using the micrometeorological aerodynamic technique, and negative values indicate evasion from the surface.

|               | Number<br>of days<br>per<br>season | Estimated<br>cumulative<br>dew depth<br><br>[mm] | Rainfall<br>depth<br>(2008)<br><br>[mm] | Estimated<br>seasonal<br>Hg<br>deposition<br>in dew<br><br>[ng m <sup>-2</sup> ] | Seasonal<br>Hg<br>deposition<br>in rain<br>(2008)<br><br>[ng m <sup>-2</sup> ] | Estimated<br>seasonal<br>atmospheric<br>dry GEM<br>deposition<br><br>[ng m <sup>-2</sup> ] |
|---------------|------------------------------------|--|---|--|--|--|
| <b>Summer</b> | 94                                 | 6.7  | 336.5                                   | 24.2   | 2983   | -5640  |
| <b>Fall</b>   | 90                                 | 3.2  | 324.8                                   | 16.6   | 1344   | -648   |
| <b>Winter</b> | 90                                 | 3.2  | 242.4                                   | 31.1   | 1177   | -8856  |
| <b>Spring</b> | 92                                 | 6.5  | 492.2                                   | 50.8   | 6878   | 10598  |
| <b>Year</b>   | 366                                | 19.6   | 1395.9                                  | 122.7  | 12382  | -4546  |

**REFERENCES: CHAPTER 3**

- Baldocchi, D. D., B. B. Hicks, and T. P. Meyers (1988), Measuring biosphere-atmosphere exchanges of biologically related gases with micrometeorological methods, *Ecology*, 69(5), 1331-1340.
- Converse, A. D., A. R. Riscassi, and T. M. Scanlon (submitted), Seasonal variability in gaseous mercury fluxes measured in a high-elevation meadow.
- de Bruin, H. A. R., R. J. Ronda, and B. J. H. Van De Wiel (2000), Approximate solutions for the Obukhov length and the surface fluxes in terms of bulk Richardson numbers, *Boundary-Layer Meteorology*, 95(1), 145-157.
- Edwards, G. C., P. E. Rasmussen, W. H. Schroeder, D. M. Wallace, L. Halfpenny-Mitchell, G. M. Dias, R. J. Kemp, and S. Ausma (2005), Development and evaluation of a sampling system to determine gaseous Mercury fluxes using an aerodynamic micrometeorological gradient method, *Journal of Geophysical Research-Atmospheres*, 110(D10).
- EPA (2002), Method 1631, Revision E: Mercury in water by oxidation, purge and trap and cold vapor atomic fluorescence spectrometry, edited.
- Fritsche, J., G. Wohlfahrt, C. Ammann, M. Zeeman, A. Hammerle, D. Obrist, and C. Alewell (2008), Summertime elemental mercury exchange of temperate grasslands on an ecosystem-scale, *Atmospheric Chemistry and Physics*, 8(24), 7709-7722.
- Garratt, J. R. (1992), The atmospheric boundary layer, 316 pp., Cambridge University Press.
- Garratt, J. R., and M. Segal (1988), On the contribution of atmospheric moisture to dew formation, *Boundary-Layer Meteorology*, 45(3), 209-236.
- Holtslag, A. A. M., and H. A. R. de Bruin (1988), Applied modeling of the nighttime surface-energy balance over land, *Journal of Applied Meteorology*, 27(6), 689-704.
- Jacobs, A. F. G., A. Vanpul, and R. M. M. Elkilani (1994), Dew formation and the drying process within a maize canopy, *Boundary-Layer Meteorology*, 69(4), 367-378.
- Jacobs, A. F. G., B. G. Heusinkveld, R. J. W. Kruit, and S. M. Berkowicz (2006), Contribution of dew to the water budget of a grassland area in the Netherlands, *Water Resources Research*, 42(3).

- Kidron, G. J. (2000), Analysis of dew precipitation in three habitats within a small arid drainage basin, Negev Highlands, Israel, *Atmospheric Research*, 55(3-4), 257-270.
- Kolker, A., M. A. Engle, W. H. Orem, J. E. Bunnell, H. E. Lerch, D. P. Krabbenhoft, M. L. Olson, and J. D. McCord (2008), Mercury, trace elements and organic constituents in atmospheric fine particulate matter, Shenandoah National Park, Virginia, USA: A combined approach to sampling and analysis, *Geostandards and Geoanalytical Research*, 32, 279-293.
- Mahaffey, K. R., G. E. Rice, and J. Swartout (1997), Mercury Study Report to Congress: An Assessment of Exposure to Mercury in the United States, EPA: Office of Air Quality Planning and Standards and Office of Research and Development, pp. 1-293, Washington.
- Malcolm, E. G., and G. J. Keeler (2002), Measurements of mercury in dew: Atmospheric removal of mercury species to a wetted surface, *Environmental Science & Technology*, 36(13), 2815-2821.
- McMillen, R. T. (1988), An eddy-correlation technique with extended applicability to non-simple terrain, *Boundary-Layer Meteorology*, 43(3), 231-245.
- Moro, M. J., A. Were, L. Villagarcia, Y. Canton, and F. Domingo (2007), Dew measurement by Eddy covariance and wetness sensor in a semiarid ecosystem of SE Spain, *Journal of Hydrology*, 335(3-4), 295-302.
- Mulawa, P. A., S. H. Cadle, F. Lipari, C. C. Ang, and R. T. Vandervennet (1986), Urban dew - its composition and influence on dry deposition rates, *Atmospheric Environment*, 20(7), 1389-1396.
- National Atmospheric Deposition Program (NRSP-3), 2009. NADP Program Office, Illinois State Water Survey, 2204 Griffith Dr., Champaign, IL 61820.
- Poissant, L., M. Pilote, C. Beauvais, P. Constant, and H. H. Zhang (2005), A year of continuous measurements of three atmospheric mercury species (GEM, RGM and Hg-p) in southern Quebec, Canada, *Atmospheric Environment*, 39(7), 1275-1287.
- Schroeder, W. H., and J. Munthe (1998), Atmospheric mercury - An overview, *Atmospheric Environment*, 32(5), 809-822.

- Sheu, G. R., and R. P. Mason (2001), An examination of methods for the measurements of reactive gaseous mercury in the atmosphere, *Environmental Science & Technology*, 35(6), 1209-1216.
- Skarzynska, K., Z. Polkowska, and J. Namiesnik (2006), Sample handling and determination of physico-chemical parameters in rime, hoarfrost, dew, fog and cloud water samples - a review, *Polish Journal of Environmental Studies*, 15(2), 185-209.
- Swartzendruber, P. C., D. A. Jaffe, E. M. Prestbo, P. Weiss-Penzias, N. E. Selin, R. Park, D. J. Jacob, S. Strode, and L. Jaegle (2006), Observations of reactive gaseous mercury in the free troposphere at the Mount Bachelor Observatory, *Journal of Geophysical Research-Atmospheres*, 111(D24), 12.
- Takenaka, N., H. Soda, K. Sato, H. Terada, T. Suzue, H. Bandow, and Y. Maeda (2003), Difference in amounts and composition of dew from different types of dew collectors, *Water Air and Soil Pollution*, 147(1-4), 51-60.
- Valente, R. J., C. Shea, K. L. Humes, and R. L. Tanner (2007), Atmospheric mercury in the Great Smoky Mountains compared to regional and global levels, *Atmospheric Environment*, 41(9), 1861-1873.
- Wagner, G. H., and K. F. Steele (1992), Dew and frost chemistry at a midcontinent site, United-States, *Journal of Geophysical Research-Atmospheres*, 97(D18), 20591-20597.
- Webb, E. K., G. I. Pearman, and R. Leuning (1980), Correction of flux measurements for density effects due to heat and water-vapor transfer, *Quarterly Journal of the Royal Meteorological Society*, 106(447), 85-100.
- Weiss-Penzias, P., M. S. Gustin, and S. N. Lyman (2009), Observations of speciated atmospheric mercury at three sites in Nevada: Evidence for a free tropospheric source of reactive gaseous mercury, *Journal of Geophysical Research-Atmospheres*, 114.
- Wolfe, M. F., S. Schwarzbach, R. A. Sulaiman, and Yu (1998), Effects of mercury on wildlife: A comprehensive review, *Environmental Toxicology and Chemistry*, 17(2), 146-160.
- Zangvil, A. (1996), Six years of dew observations in the Negev Desert, Israel, *Journal of Arid Environments*, 32(4), 361-371.

## **CHAPTER 4**

### **Conclusions and avenues for future research**

---

## ***1. Conclusions***

### *1.1 Seasonal atmospheric mercury fluxes*

Gaseous elemental mercury (GEM) fluxes were measured for weeklong periods within each of the four seasons (spring, summer, fall, and winter) in Shenandoah National Park, and exhibited significant seasonal variability. Spring appears to be an important period for net deposition (mean:  $-4.8 \text{ ng m}^{-2} \text{ h}^{-1}$ ) while all other seasons exhibited net emission (means ranging from  $0.3$  to  $4.1 \text{ ng m}^{-2} \text{ h}^{-1}$ ). Spring and summer fluxes revealed a diel pattern of deposition at night and emissions during the day. Fluxes in the winter were similar to those measured over bare soil (e.g. Stamenkovic et al., 2008) with emissions during the day and near-zero fluxes at night.

The strongest GEM deposition pattern was reported at nighttime in the spring ( $-7.3 \text{ ng m}^{-2} \text{ h}^{-1}$ ). Assuming that soils generally exhibit emission fluxes when GEM concentrations in the atmosphere are low ( $< 2 \text{ ng m}^{-3}$ ), the GEM deposition during the spring was attributed to uptake by the actively growing vegetation. Because stomata are closed at night and stomatal resistance to gaseous uptake is increased, we hypothesized that Hg was diffusing into plant cuticles. In addition, GEM fluxes were not significantly correlated to modeled canopy conductance which also suggests a nonstomatal pathway for deposition. Alternatively, it is also possible that GEM is taken up thru stomata, but not primarily limited by stomatal closure.

In the summer, nighttime GEM deposition was still detectable ( $-2.5 \text{ ng m}^{-2} \text{ h}^{-1}$ ), but was reduced in magnitude in comparison to the springtime measurements. This variability could be related to the physical structure of the plants as they age. In the summer, mercury (Hg) levels in the plants could be nearing an equilibrium state with respect to atmospheric Hg, decreasing the rate of Hg uptake. Alternatively, the increased summertime temperatures might have produced greater GEM emissions from the soil which would partially mask any deposition to vegetation.

### *1.2 Relevance of dew formation to mercury deposition*

Dew samples were collected and analyzed for Hg concentration and dew depth was calculated over the natural surface using a micrometeorological method (Jacobs et al., 2006) to estimate the relative importance of dew formation to total Hg deposition. Mercury concentrations in dew at the Big

Meadows site had a mean value of  $5.57 \pm 4.45 \text{ ng L}^{-1}$ , which was lower than mean rainfall concentration ( $8.80 \pm 7.08 \text{ ng L}^{-1}$ ). Hg deposition to dew could be limited by the amount of soluble Hg ( $\text{Hg}^{2+}$  and particular-bound) present in the atmosphere since concentrations of these species are generally low at remote, vegetated sites ( $\sim 3 \text{ ng m}^{-3}$ ; Kolker et al., 2008). Cloud droplets could scavenge Hg from higher regions of the troposphere more enriched with soluble Hg species (Swartzendruber et al., 2006) resulting in higher Hg concentrations in rainfall. There was low variability in the mass of Hg deposited for each dew event, and there was not a significant difference in the mass of Hg deposited to frost samples in comparison to liquid dew.

When Hg deposition was scaled to the annual level, estimated deposition to dew only accounted for a small fraction of the total Hg deposition relative to rainfall and dry GEM deposition. Rainfall contributed two orders of magnitude more Hg to the site, primarily because the cumulative rainfall depth ( $\sim 1400 \text{ mm}$ ) was much greater than the estimated cumulative dew depth ( $\sim 20 \text{ mm}$ ). Based on this scaling exercise, we determined that it is not necessary to account for dew deposition in Hg budgets at sites with rainfall patterns similar to Shenandoah National Park. However, it could be a significant source of aqueous Hg deposition in arid regions (e.g. Negev Desert; Zangvil, 1996) where yearly dew depths are of similar magnitude to annual precipitation.

## ***2. Avenues for future research***

### *2.1 Duration of seasonal patterns*

The GEM flux measurements at Big Meadows recorded net deposition in the spring and emission during all of the other seasons, but additional research is needed to determine if these patterns are representative of other vegetated locations with low Hg levels in the soil and the air. In addition, longer field campaigns are needed to determine the approximate duration of each of each seasonal pattern. For example, how long does the springtime deposition persist before transitioning to net summer emission? Is the timing of the transition relatively uniform across landscapes or does it significantly vary for different vegetation types?

For logistical reasons, long-term GEM flux measurement sites should be selected at locations with access to a power supply and a semi-permanent containment structure to house the Hg analyzer.

The Hg analyzer is capable of continuously running without daily monitoring and can be programmed to regularly calibrate using an internal calibration source. However, it does require periodic maintenance (e.g. changing filters every 2 weeks), and therefore the site should be easily accessible. The University of Virginia has access to several long-term research stations that meet these criteria and could be viable options for establishing a long-term GEM flux measurement study: the Virginia Coast Reserve Long-Term Ecological Research (VCR LTER) and the Pace Estate. The landscapes at these sites (tidal marsh and mixed deciduous forest, respectively) are different from those at Big Meadows (high elevation wetland meadow) offering an opportunity to observe seasonal GEM fluxes over different vegetation communities.

## *2.2. Leaf-level evidence for Hg uptake by vegetation through a stomatal or cuticular pathway*

Controlled laboratory studies at the leaf level are needed to establish if GEM enters/exits vegetation primarily through a stomatal or cuticular pathway. Experiments that isolate the stomata and astomatal leaf surface would quantitatively determine the relative fraction traveling through each pathway. GEM fluxes from the astomatal surfaces would be attributed to a cuticular pathway, while fluxes from the stomatal surfaces would be a combination of both the stomatal and cuticular pathways. It is possible that the relative importance of either pathway is specific to the plant species, or related to the age of the individual plant. To address this, leaf level studies could be conducted over a range of plant species at varying stages of growth.

Hg chamber studies can be plagued by contamination issues, therefore strict quality control procedures are required to ensure accurate GEM flux measurements. All equipment should be thoroughly cleaned and regular chamber blank measurements taken to determine if the internal surface of the chamber is scavenging or emitting Hg. GEM fluxes from a single leaf are likely to be very small, and any contamination from the measurement apparatus could mask the flux signal. Careful attention should also be given to the air source for the chamber flushing gas since this could change the magnitude of GEM fluxes. To this end, Stamenkovic and Gustin (2009) reported that GEM deposition to vegetation was reduced when ambient outside air was used as a flushing gas in comparison air scrubbed using an activated carbon filter (removes ozone and trace gases). The

presence of atmospheric oxidants could augment GEM emission from vegetation, reducing the net deposition flux.

### *2.3 Fate of Hg deposited to dew*

Simulated dew events could be completed in the laboratory to determine the fate of the Hg deposited to dew on vegetated surfaces. GEM or speciated Hg fluxes could be measured over time as the water evaporates to determine if the Hg is emitted while the water evaporates, if it is emitted more slowly, or if it remains bound to plant tissue. Alternatively, many plants could be repeatedly sprayed with artificial Hg-rich dewfall over several nights. Individual plants/leaves could be analyzed for Hg concentration to determine if Hg levels within the plant tissue are related to the number of dew-applications. Finally, dew samples could also be collected from natural surfaces to determine if Hg concentrations are significantly different from those collected from a Teflon sheet.

### **3. Acknowledgements**

I would like to express my deep thanks to the many individuals that made this research possible. My advisor, Dr. Todd Scanlon, offered continuous support and advice regarding experimental design, data processing, and interpretation. I would also like to thank my committee members, Dr. Jose Fuentes and Dr. Manuel Lerdau, for their guidance throughout the project. John and Susie Maben offered invaluable assistance in laboratory and field work, and numerous members of the National Park Service staff supported the data collection efforts at Big Meadows. And finally, I am most indebted to my lab mates, Ami Riscassi and Clara Funk, for their daily insight, encouragement, and goodwill for the duration of this research.

**REFERENCES: CONCLUSIONS**

- Jacobs, A. F. G., B. G. Heusinkveld, R. J. W. Kruit, and S. M. Berkowicz (2006), Contribution of dew to the water budget of a grassland area in the Netherlands, *Water Resources Research*, 42(3).
- Kolker, A., M. A. Engle, W. H. Orem, J. E. Bunnell, H. E. Lerch, D. P. Krabbenhoft, M. L. Olson, and J. D. McCord (2008), Mercury, trace elements and organic constituents in atmospheric fine particulate matter, Shenandoah National Park, Virginia, USA: A combined approach to sampling and analysis, *Geostandards and Geoanalytical Research*, 32, 279-293.
- Stamenkovic, J., and M. S. Gustin (2009), Nonstomatal versus stomatal uptake of atmospheric mercury, *Environmental Science and Technology*, 43(5), 1367-1972.
- Stamenkovic, J., M. S. Gustin, J. A. Arnone, D. W. Johnson, J. D. Larsen, and P. S. J. Verburg (2008), Atmospheric mercury exchange with a tallgrass prairie ecosystem housed in mesocosms, *Science of the Total Environment*, 406(1-2), 227-238.
- Swartzendruber, P. C., D. A. Jaffe, E. M. Prestbo, P. Weiss-Penzias, N. E. Selin, R. Park, D. J. Jacob, S. Strode, and L. Jaegle (2006), Observations of reactive gaseous mercury in the free troposphere at the Mount Bachelor Observatory, *Journal of Geophysical Research-Atmospheres*, 111(D24), 12.
- Zangvil, A. (1996), Six years of dew observations in the Negev Desert, Israel, *Journal of Arid Environments*, 32(4), 361-371.